Laflin, J. M. and A. L. Houston, 2012: A modeling study of supercell development in the presence of a preexisting airmass boundary. *Electronic J. Severe Storms Meteor.*, **7** (1), 1–29.

Electronic Journal of
SEVERE STORMS METEOROLOGY

A Modeling Study of Supercell Development in the Presence of a Preexisting Airmass Boundary

JENNIFER M. LAFLIN AND ADAM L. HOUSTON
University of Nebraska-Lincoln, Lincoln, Nebraska

(Submitted 18 May 2011; in final form 19 January 2012)

ABSTRACT

Airmass boundaries have been documented as a major influence on convective initiation and development, particularly in supercell thunderstorms. Therefore, this study seeks to determine the specific influence of an airmass boundary on supercell development through idealized numerical modeling. To do this, convective initiation is simulated in an environment that represents a case where supercells were observed forming along a preexisting airmass boundary. Three simulations are conducted, which illustrate convective initiation in the warm sector, cool sector, and along the airmass boundary. Deep convection occurs in all simulations; however, a steady-state supercell is only produced in the boundary simulation. Analysis of these results reveals that the airmass boundary supports supercell formation and development by increasing the strength of the updraft, creating and supporting a low-level mesocyclone, and enhancing the gust front. In this study, the airmass boundary is found to have a profound impact on the simulated storm, and is necessary for supercell development and longevity even with an ambient environment that supports supercells.

1. Introduction

A supercell (Browning 1964) is defined by having a deep, persistent mesocyclone (Moller et al. 1994; Doswell 2001). Supercells have been related to a majority of the significant severe weather associated with deep convection, defined as hail ≥5.1 cm in diameter, nontornadic wind gusts ≥33 m s^{-1} and significant tornadoes (EF2 and greater), and account for a large portion of damage which results from thunderstorms (Moller et al. 1994; Doswell 2001). Advanced warning of severe weather is necessary to protect life and property; and for this reason, it is important to recognize the mechanisms and environments that tend to produce supercells. A number of studies have focused on environments that favor the development of supercells or, rather, the formation of a supercell from existing deep convection (e.g., Weisman and Klemp 1982; Rasmussen and Blanchard 1998; Thompson et al. 2003). For example, moderate CAPE, high values of environmental shear, and low convective inhibition (CIN) often are found where supercells develop (Rasmussen and Blanchard 1998; Thompson et al. 2003). Storm-relative helicity (SRH; Davies-Jones 1984) also has been shown to have utility in differentiating between supercellular and nonsupercellular environments. In addition, parameters have been developed that combine shear and CAPE and can discriminate between convective modes, such as the energy-helicity index (Hart and Korotky 1991; Davies 1993), the bulk Richardson number (BRN; Weisman and Klemp 1982), the vorticity generation parameter (Rasmussen and Blanchard 1998), and the supercell composite parameter (SCP; Thompson et al. 2003; summarized at http://www.spc.noaa.gov/exper/mesoanalysis/help/help_scp.html), among others.

The use of parameters from these studies in operational forecasting has led to the creation of thresholds or benchmark values to distinguish between convective modes; by calculating the values of these parameters, an environment can be diagnosed as

Corresponding author address: Jennifer M. Laflin, NOAA/National Weather Service, 26 Weather Lane, Sioux Falls, SD 57104.
E-mail: jennifer.laflin@noaa.gov

supportive or unsupportive of supercells. However, these values frequently are flawed, in that the soundings from which they were calculated may not be representative of the storm's environment (Houston et al. 2008). In addition, it is also important to recognize mechanisms that alter environments to support supercells. Optimal values of CAPE and environmental shear can be created by a favorable synoptic pattern; however, mesoscale features such as an airmass boundary can enhance an environment that is marginally supportive, or even unsupportive, of supercells on a larger scale (Markowski et al. 1998). While the introduction of a mesoscale feature may create more favorable values for parameters such as vertical wind shear, it also can enhance the environment in ways that are not captured through parcel theory, such as locally enhanced vertical motion or additional environmental vertical vorticity.

An airmass boundary, most simply defined as a demarcation between two airmasses with different densities, has profound implications for convection. Several properties of an airmass boundary help to support both storm longevity and rotation in thunderstorms, thus enhancing an environment to support supercells. Forced ascent along the boundary creates lift which strengthens the storm's updraft and assists with storm maintenance and longevity. With low CAPE or a large area of CIN near the surface, this area of ascent could promote updraft maintenance in an environment that otherwise may be detrimental to the storm. A relative enhancement of moisture also may be present along boundaries (Maddox et al. 1980), which lowers the lifted condensation level (LCL) and level of free convection. This moisture also can extend into the mid levels, decreasing the chance for parcel dilution (Houston and Niyogi 2007).

In addition to forced ascent and moisture enhancement, boundaries also generate horizontal vorticity. The two primary ways that horizontal vorticity is generated along an airmass boundary are: 1) through a vertical pressure gradient at the head of the boundary, which is quantified by the solenoidal term of the horizontal vorticity tendency equation, and 2) in the cooler air mass, by enhanced vertical shear created by backing winds due to the environment's attempt to reach thermal wind balance (Maddox et al. 1980). Environments with low vertical shear—and thus low ambient horizontal vorticity—can be enhanced by additional horizontal vorticity along an airmass boundary, creating the potential for the development of a mesocyclone. Enhanced positive vertical vorticity along the boundary, whether generated through stretching of preexisting vertical vorticity along the boundary or tilting and stretching of horizontal vorticity found in the denser side of the boundary, can supplement the mesocyclone directly as it interacts with a boundary environment (Schlesinger 1975; Klemp and Wilhelmson 1978).

The connection between supercell development and airmass boundaries has been documented in a number of previous studies (Maddox et al. 1980; Markowski et al. 1998; Atkins et al. 1999; etc.). Atkins et al. (1999) found that a low-level mesocyclone is longer-lived and stronger when the storm encounters an airmass boundary. In addition, their study hypothesized that the mechanism for low-level mesocyclogenesis is fundamentally different in the presence of an airmass boundary. By observing two cases in which tornadic thunderstorms formed in non-outbreak environments, Maddox et al. (1980) suggested that both a local increase in moisture convergence along the boundary and changes to relative vertical vorticity in the boundary layer support the intensification of thunderstorms over boundaries. Markowski et al. (1998), in an overview of tornadic supercells associated with boundaries during VORTEX-95, suggested that horizontal vorticity enhancement—such as that created by an airmass boundary—is necessary for low-level mesocyclogenesis, with the exception of extremely favorable conditions, such as a tornado outbreak day. Based on the results of these studies, it is apparent that airmass boundaries can be important for supercell development, both in supercellular environments and as a local enhancement to otherwise nonsupercellular environments.

Although previous studies have examined the impact of an airmass boundary on the low-level mesocyclone, the role of the cooler air mass in the development of the midlevel mesocyclone has not been discussed. The simulated airmass boundary also has been considered a static entity and trajectories are only calculated at one time; therefore, it is not possible to address how the boundary and surrounding air masses are contributing as the mesocyclone develops. This study seeks additional insight on how the influence of the airmass boundary on storms changes throughout the storm's life cycle, and also analyzes the role of the cooler air mass by using that airmass as a control experiment. In addition, while previous research has addressed the role of airmass boundaries in mesocyclogenesis, the individual contributions of additional horizontal vorticity or enhanced vertical velocity from forced ascent have not been attributed to supercell development. A theoretical argument can be made for how airmass boundaries could support supercell development using the vorticity tendency

equation; however, these processes have not been observed separately. Strictly observational studies do not allow for comparison to a control experiment, therefore it is impossible to know how storms would develop without a boundary present. High-resolution numerical modeling, however, allows for a control simulation, as well as high spatial and temporal resolution of multiple variables, and a detailed diagnosis of the boundary and surrounding environment. Through the use of storm-scale numerical modeling, this study investigates the specific properties of an airmass boundary that support supercell development, and examines the individual contributions of these properties.

To isolate the role of the airmass boundary on supercell development, convection was simulated both in an environment which included an airmass boundary, and in homogeneous environments that served as control simulations. The boundary simulation allowed analysis of both the boundary and the evolution of the simulated storm as it interacted with the boundary. The homogeneous simulations allowed comparison of mesocyclone strength and longevity between the storms produced in the boundary versus homogeneous environments. These simulations were based on a supercell which formed along an outflow boundary in the Texas Panhandle on 25 May 1999. Homogeneous environments from the warm and cool sides of the boundary, and a representation of the actual environment with a boundary present, were simulated. Detailed analyses of these simulations then were performed to determine the specific influence of the preexisting airmass boundary on supercell formation and morphology. It was found that the airmass boundary has three main impacts on the simulated storm: 1) enhancement of the updraft by forced ascent along the boundary, which allows a stronger right-splitting storm to develop, 2) production of a forward-flank gust front (hereafter, gust front) through a combination of storm outflow and the cool air mass, which allows the storm to transition away from precipitation and continually draw in warm air, and 3) provision of enhanced horizontal vorticity that supports the development and maintenance of a low-level mesocyclone.

2. Methodology and environment

To study the effect of a preexisting airmass boundary on supercell formation, deep, moist convection was simulated in three environments: one entirely representing the warm (less dense) side of a boundary, one representing just the cool (denser) side of a boundary, and one containing a boundary. The model initially was prescribed by a sounding taken from North American Regional Reanalysis (NARR; Mesinger et al. 2006) data at 2100 UTC on 25 May 1999. This environment was chosen for model initialization due to the presence of several outflow boundaries (Fig. 1) and the observation of supercell development along or near these boundaries shortly before 2100 UTC, and was also documented in a case study describing the boundaries and a supercell that traveled along the preexisting outflow (Dostalek et al. 2004). An airmass boundary was resolved in NARR data near the observed location of the outflow boundaries (Fig. 2), which validated the use of NARR data for model initialization and allowed for a comparison of the warm- and cool-side environments.

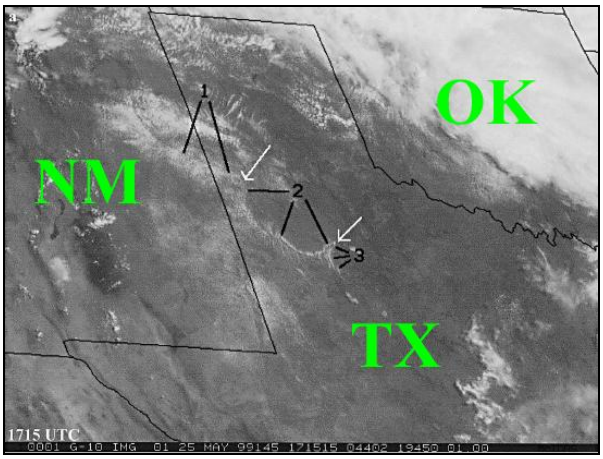

Figure 1: GOES-10 visible satellite image of cloud arcs accompanying outflow boundaries at 1715 UTC on 25 May 1999, adapted from Dostalek et al. (2004). *Click image to enlarge.*

The warm-side sounding and wind profile used for model initialization (Figs. 3 and 4) were interpolated from the NARR at a point ≈30 km away from the boundary in the warm side. The time used for the proximity sounding was 2100 UTC, which is ≈1 h after convection initiated along the outflow boundary. Rawinsondes were launched on 25 May 1999 at 1200 UTC and 1800 UTC by the National Weather Service in Amarillo, TX and at 1200 UTC in Midland, TX. Neither sounding was located in sufficient proximity to the outflow boundary to represent the warm-side environment; thus, model data were required to represent the appropriate environment. To identify the outflow boundary characteristics such as its depth, as well as the temperature, moisture, and wind profiles, another proximity sounding was taken at a point 30 km into the cool side, and was compared to the warm-side proximity sounding.

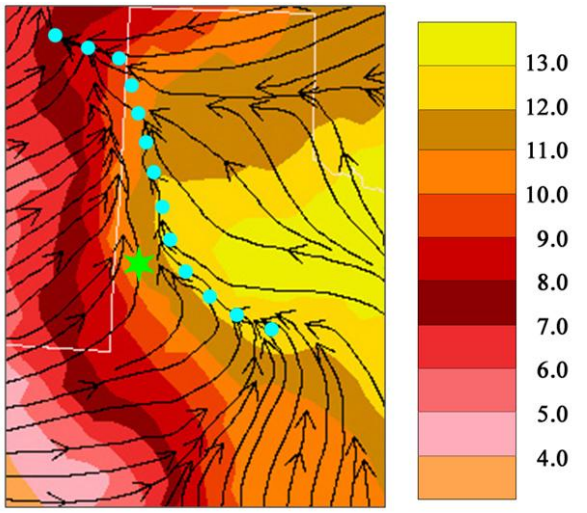

Figure 2: NARR 2-m mixing ratio in g kg^{-1} (shaded per legend), 10-m streamlines (black), and approximate location of the airmass boundaries (cyan dotted line) and the warm-side sounding location (green star).

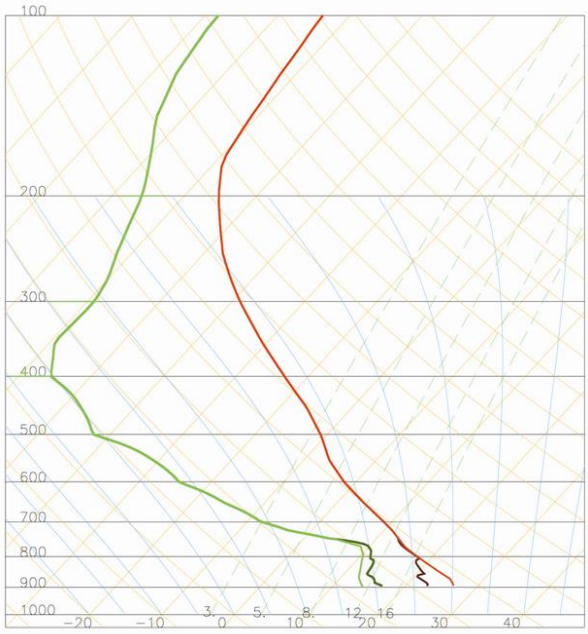

Figure 3: Skew *T*–log*p* diagram of the warm-side (light green and red) and cool-side (green and dark red) soundings used to initialize the homogeneous simulations. The warm-side sounding is taken from NARR data, while the cool-side sounding is a point sounding from the boundary simulation.

For initialization of the homogeneous simulation representing the cool side of the boundary, a sounding was taken from the *boundary simulation* ≈30 km into the cool side. Although the density current was prescribed to best represent the boundary observed both in the NARR and surface observations, the simulated cool-side environment and the cool-side proximity sounding from the NARR were not identical. In order to maintain consistency with the environment in the boundary simulation, it was necessary to use a sounding from the cool side (Figs. 3 and 4) for initialization there. In contrast to the warm and cool-side simulations that were horizontally homogeneous at model initialization, the simulation representing the boundary environment was created by the warm-side sounding with the addition of an outflow boundary covering the northern half of the domain.

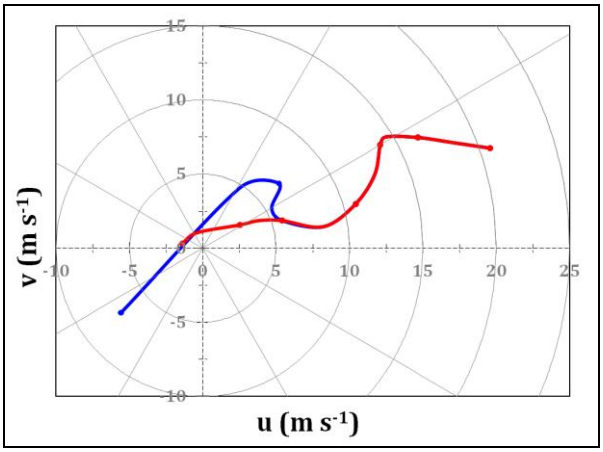

Figure 4: 0–6-km AGL hodographs for the warm-side (red) and cool side (blue) used to initialize the homogeneous simulations, adapted from M. Bunkers' program (http://www.crh.noaa.gov/images/unr/soo/scm/Hodograph_Spreadsheet.xls). Tick marks are every 1 km.

As an initial prediction of whether to expect supercells or nonsupercells in the homogeneous simulations, mean-layer (ML) CAPE, MLCIN, environmental bulk wind differential (BWD), storm-relative helicity, and the SCP were computed from both the warm-side and cool-side soundings and compared to expected values for supercell environments, such as those found by Rasmussen and Blanchard (1998) and Thompson et al. (2003). A summary of these values, as well as typical values for a supercell environment (Thompson et al. 2003), can be found in Table 1. On the warm side of the boundary, the CAPE and CIN were well within the expected range for supercells; however, the shear was marginal, resulting in borderline values for 0–6-km AGL BWD and the SCP, and nonsupercellular values for 0–3-km AGL SRH (calculated using observed storm motion of the right-

splitting storm in the warm simulation and the left-splitting storm in the cool simulation). In addition, the sounding was quite dry throughout the profile depth, and a low-moisture environment potentially can lead to dilution and a decrease in the overall instability of the parcel (Ziegler and Rasmussen 1998; Houston and Niyogi 2007). Values on the cool side were closer to what would be expected in a supercell environment, with supercellular values of 0–6 km AGL bulk shear, SCP, and CAPE, and a marginal value of 0–3-km SRH. However, the moderate value of MLCIN, as well as the more negative value of surface-based CIN (–110 J kg^{-1}), would have made it extremely difficult for surface-based convection to develop without some external forcing.

Table 1: Selected severe weather parameters for the homogeneous environments, compared to marginal values for a supercell environment (Rasmussen and Blanchard 1998; Thompson et al. 2003).

	Warm	Cool	Supercell
MLCAPE (J kg^{-1})	2251	1924	≥1000
MLCIN (J kg^{-1})	–7	–59	≥–70
0–6 km BWD (m s^{-1})	21.6	27.8	≥20
0–3 km Helicity (m^{-2} s^{-2})	25	–107	≥±100
SCP	1.29	6.50	≥1.0

Idealized modeling was used to simulate deep convection, in order to isolate the role of the preexisting airmass boundary on the development of the mesocyclone. The idealized modeling platform excludes other factors that may have a role in modifying the storm's convective mode, such as radiation, evapotranspiration, or surface friction, while also allowing a thorough and detailed analysis of the airmass boundary and simulated storms. The model used in this study is the Illinois Collaborative Multiscale Model for Atmospheric Simulations (ICOMMAS; Houston 2004), a non-hydrostatic, finite-difference model. ICOMMAS is similar to its predecessor, COMMAS (Wicker and Wilhelmson 1995), but was designed specifically to study the relationship between convective initiation and airmass boundaries. In the horizontal plane, open lateral boundary conditions were selected, which treated any distance outside the domain as a reflection of the simulated domain (Klemp and Wilhelmson 1978). The microphysics scheme used was a single moment, three-phase ice parameterization (Gilmore et al. 2004). Simulations were completely idealized and therefore did not include a land surface model, surface layer scheme, or an atmospheric radiation scheme.

In order to capture the supercellular nature of a thunderstorm while limiting simulations to reasonable computational time and resources, a grid spacing of 500 m was used in the horizontal, with a vertical grid spacing ranging from 100 m in the boundary layer to 500 m in the upper troposphere. Although somewhat coarser than the 100–250-m grid spacing suggested by Bryan et al. (2003), this grid spacing resembles those used in other studies which consider phenomena on a similar scale (Adlerman et al. 1999; Atkins et al. 1999; Houston 2004). The full model domain was 80 km in both horizontal directions by 19.5 km in the vertical. The NARR sounding used to initialize the model had a maximum height of approximately 19.8 km, which limited the depth of the domain. In addition, the grid was translated at each time step to follow the storm, which allowed a relatively small horizontal domain.

To create the airmass boundary, an 1100-m deep block of cold air was introduced into the warm-side environment, covering the northern half of the domain. Initially, the temperature perturbation inside the density current was a constant –4 K, and the water vapor mixing ratio perturbation decreased from 2.1 g kg^{-1} at the surface to 1.0 g kg^{-1} at the top. This initial block of cold air was unrepresentative of an actual boundary, since the moisture profile had no gradient or variation in the horizontal, and the temperature profile did not vary in the horizontal or vertical directions. To mitigate this effect, the environment was initialized first in a shallow domain (1500 m deep). The LCL of the warm-side base state was 1595 m AGL, so the shallow domain allowed the environment to adjust without initiating convection. After 3600 s of adjustment, the shallow domain (Fig. 5) was seeded into the full three-dimensional domain, as described in Houston and Niyogi (2007). At this point in the procedure, deep moist convection could develop, but precipitation did not form. Instead of the boundary itself initiating convection, a thermal bubble was used.

For all simulations, a thermal bubble with a horizontal radius of 10 km and a vertical radius of 750 m was used to initiate convection. A 3 K perturbation was present in the center of the bubble, which decreased to zero on the edges. The bubble was centered at 750 m AGL in the warm-side and boundary simulations, and at 1.5 km AGL in the cool side. simulation. In the cool-side simulation, the stable layer created by the airmass boundary had the potential to

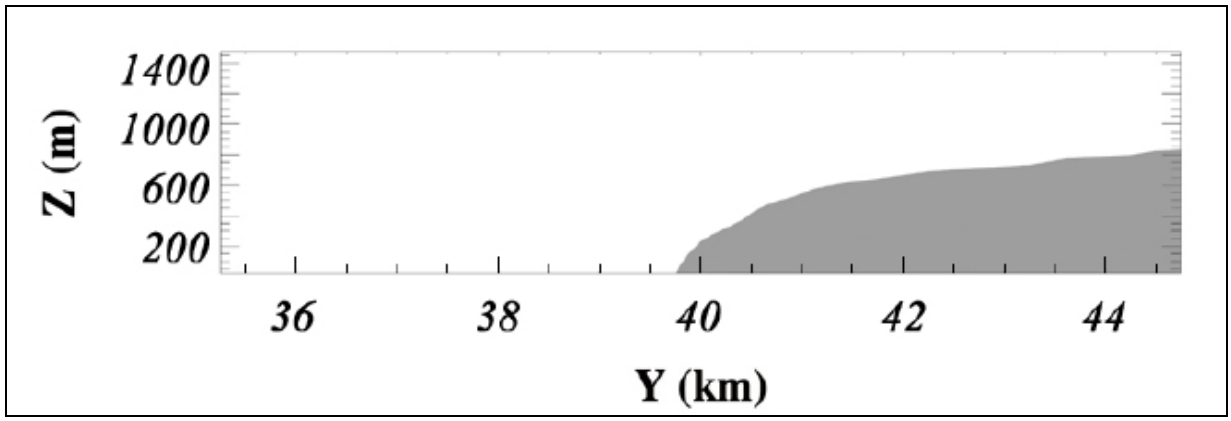

Figure 5: The simulated outflow boundary in the channel domain before being seeded into the full domain at 3600 s. Shading is potential temperature perturbation <0 K.

inhibit convection, since it created a large value of CIN for parcels originating from the surface. To mitigate this and more accurately represent the process of elevated inflow to a storm located above a shallow stable air mass, the thermal bubble for convective initiation was based above the stable layer. The simulation containing a boundary was initialized with a slab-symmetric density current containing temperature and water vapor mixing ratio perturbations that were prescribed to best resemble the boundary observed in the selected case study. The same thermal bubble that initiated convection in homogeneous simulations was used in the boundary simulation, instead of allowing convective initiation along the boundary itself. This was done to represent a preferential location for convective initiation along the boundary, and to prevent convection from forming in a line throughout the length of the domain. Due to the environmental wind profile, the boundary and bubble had different propagation speeds; therefore, in the boundary simulation, the bubble was positioned on the warm side of the domain, so that the storm began producing precipitation as it entered the boundary environment.

3. Results

The results of the simulations are presented in three subsections: time-series analysis, storm-split analysis, and trajectory analysis. Time-series analyses provide an overview of the timing and progression of precipitation at the surface, vertical vorticity, and updraft strength, in order to create associations and draw preliminary connections between the environments and simulated storms (section 3a). Early in the boundary simulation, the right-moving storm experienced a major transition after a split. The processes that lead to the split and the impacts of the split on the simulated storm are described in detail in the storm-splitting analysis section (3b). As a final method of analyzing the results, trajectories were computed in the boundary simulation to determine the source regions of vertical vorticity in the mesocyclone, and to serve as a detailed method of examining the impact of the boundary on the simulated storm's progression and overall strength throughout its life cycle (3c). In this study, trajectories were initialized in a vertical slice within an area of interest, such as the midlevel mesocyclone or low-level (cloud base; ≈1.5 km AGL) updraft, and then were integrated backwards in time to determine the position of each tracer at preceding times. Plan-view images of trajectory paths use different colors to signify the height of the trajectory through time, allowing a comparison of the trajectory's track to a vertical slice at a specified time. In addition to those plan views, numerous variables can be calculated for each trajectory at any given time. Time series and vertical profiles of specific variables then can be plotted and analyzed for trajectories.

a. Time-series analysis

For the purpose of comparison in the time-series analysis, a storm was considered to have mesocyclonic rotation when the vertical vorticity in that storm reached or exceeded a magnitude of 0.01 s^{-1}. The storm still was not considered a supercell until reaching the time constraint (mesocyclonic rotation for >~30 min; Moller et al. 1994, Doswell 2001) in addition to the vorticity threshold; however, for the sake of comparison between simulations, vertical vorticity was measured at each time step. A proxy for radar reflectivity was calculated from model-derived mixing ratios of rain and hail (Smith et al. 1975), resulting in values comparable to those from the Weather

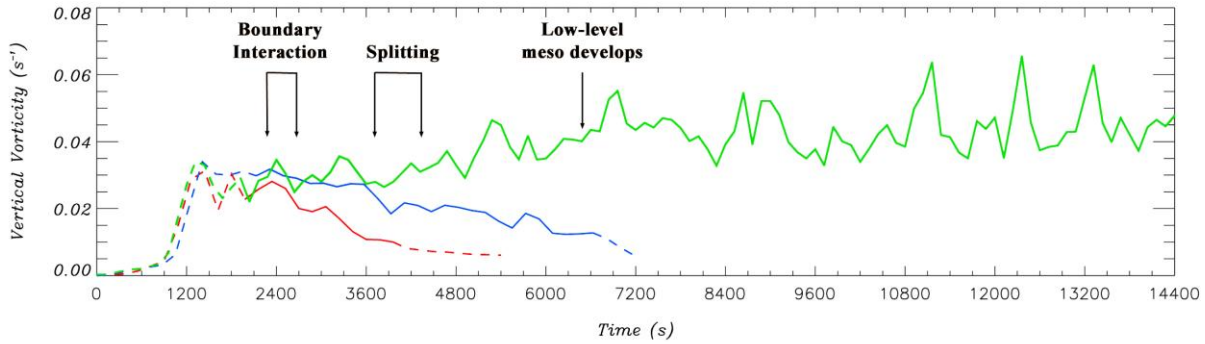

Figure 6: Time series of the maximum magnitude of vertical vorticity throughout the depth of the domain for the boundary (green), cool-side (blue), and warm-side (red) simulations. Dashes indicate that the storm does not meet mesocyclone criteria, either because precipitation has not yet reached the surface or the magnitude of vertical vorticity is $\leq$0.01 s^{-1}. Annotations on the figure apply only to the boundary simulation. *Click image to enlarge.*

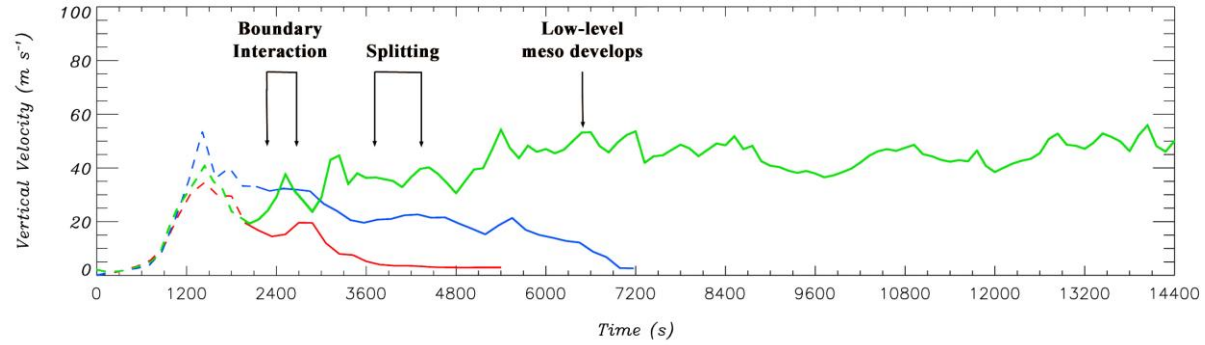

Figure 7: Same as in Fig. 6, except for maximum vertical velocity. Dashed lines indicate that precipitation has not yet reached the surface. *Click image to enlarge.*

Surveillance Radar 88-Doppler, and was used to analyze and compare model simulation results. Plots of simulated reflectivity were used as a supplement in the time-series analysis, in order to provide an overview of the simulated storm's structure and progression throughout its life cycle.

The warm-side simulation was run for 2 h, with the thermal bubble released at 0 s. The lifetime of the simulated storm (surface precipitation present) was 39 min, while mesocyclonic rotation was present for 30 min (Table 2); the maximum vertical vorticity found in this storm was $\approx$0.03 s^{-1} and was present in the first 10 min of the mesocyclone's lifetime (Fig. 6). The main updraft pulsed upward in intensity early in the simulation, then generally decreased in strength thereafter (Fig. 7). Contours of vertical vorticity featured multiple areas of midlevel rotation and the quick immersion of these mesocyclones into precipitation (Fig. 8). Due to the presence of mesocyclonic rotation at mid levels for 30 min, the storm produced in the warm-side simulation could be considered a supercell, although transient and very short lived.

The cool-side simulation also was run for 2 h, with the thermal bubble released at 0 s. Surface precipitation was present for 85 min. The magnitude of vertical vorticity exceeded 0.01 s^{-1} at the mid levels on both flanks of the storm when precipitation initially reached the surface (Fig. 9). At first, low-level rotation was absent on either flank; however, mesoanticyclonic rotation developed at cloud base ($\approx$1 km) on the left flank $\approx$10 min later. The low-level rotation persisted for 15 min and splitting occurred 3 min later, around the time of the right flank rotation's demise. In this

simulation, the left split contained a mesoanticyclone which persisted for 78 min, while the cyclonic rotation in the right-splitting storm lasted 27 min (Table 2). The dominance of the left-moving split likely is due to the shape of the hodograph (Fig. 4), which also was observed by Dostalek et al. (2004). Vertical-vorticity magnitudes for the left-splitting storm in the cool-side simulation were similar to those in the warm-side simulation, with a maximum magnitude of ≈0.03 s^{-1} occurring early, and an overall decrease throughout the remainder of the storm's lifetime (Fig. 6). Although the updraft in the cool-side simulation was stronger than the warm-side simulation and peaked at a value of 53 m s^{-1} before precipitation formed, the same overall decreasing trend could be observed in both simulations (Fig. 7).

Table 2: Start and end times of the midlevel mesocyclone in seconds for each simulation, and the lifetime of each mesocyclone in minutes (asterisk denotes mesoanticyclone lifetime).

	Start (s)	End (s)	Life (min)
Warm	1980	3780	30
Cool	2130	6810	27 (78*)
Boundary	1920	14400	208

The storm produced in the boundary simulation is the final storm to be described in this section. After the boundary stabilized in the channel domain and was seeded into the full domain (3600 s), a thermal bubble was released—this then is defined[1] as time = 0 s. The thermal bubble was placed on the warm side of the boundary, so that the simulated updraft encountered the forced ascent along the boundary just as precipitation began reaching the surface. Surface precipitation and mesocyclonic rotation both persisted throughout the length of the simulation (Fig. 6), which was terminated at 14 400 s—4 h after the thermal bubble was released and approximately 3.5 h after precipitation first reached the surface (Table 2).

The storm split into left- and right-moving components ≈40 min after the bubble was released, and both contained midlevel vortices; however, the right mover became dominant and contained a low-level mesocyclone for almost 2 h (Fig. 10). The weaker left-moving storm moved out of the domain approximately 2.5 h into the simulation, which was allowed so that the dominant right-moving storm could remain near the center of the domain. Vertical-vorticity magnitudes were maximized at 0.03 s^{-1} in association with the left-moving storm, while maximum vertical-vorticity values of 0.065 s^{-1} were associated with the right-moving storm (Fig. 6). Unlike previous simulations, both vertical vorticity and vertical velocity showed an increasing and then steady trend of relatively high values throughout the simulation for the right mover. Vertical velocity generally increased through the first 2 h, with some variation as the storm organized, then remained around 50 m s^{-1} throughout the remainder of the simulation (Fig. 7). In this simulation, both the left- and right-moving storms contained a mesoanticyclone or mesocyclone, respectively, and the right-moving storm became a long-lived, persistent supercell.

The development of the updraft at early stages was complicated by the presence of the airmass boundary. When compared to the homogeneous warm side, the updraft in the boundary simulation began to increase beyond values seen in the homogeneous simulation as early as 1260 s (Fig 11); however, the updraft was not superimposed with the vertical motion along the boundary until 2280 s (Fig. 12). Although the main updraft did not encounter the forced ascent of the boundary directly until 2280 s, other effects of the boundary, such as enhanced inflow, helped to strengthen the updraft well before this time. This accounts for the differences between the homogeneous and boundary simulations. The boundary environment can be defined loosely as the area from 10 km into the warm side to 30 km into the cool side (Markowski et al. 1998), so it is unsurprising that the boundary storm experienced some enhancement before directly encountering the forced ascent. In order to examine how far into the warm side the boundary environment extended, convergence, wind direction, and θ_e were plotted, along with vertical wind speed, for a tracer that was lifted by forced ascent along the boundary (Fig. 13). To avoid sampling any storm-related contamination of the homogeneous environment, the trajectory was calculated ≈30 km east of the bubble release. Changes to the homogeneous environment were apparent as far as 10 km into the warm side, which occurred well before the parcel was lifted above ground level. By 1260 s, the leading edge of the thermal bubble was centered ≈5 km south of the boundary, or well within the boundary environment.

[1] All times described in this section, as well as the times used on all time series and images, refer to elapsed time from the bubble release.

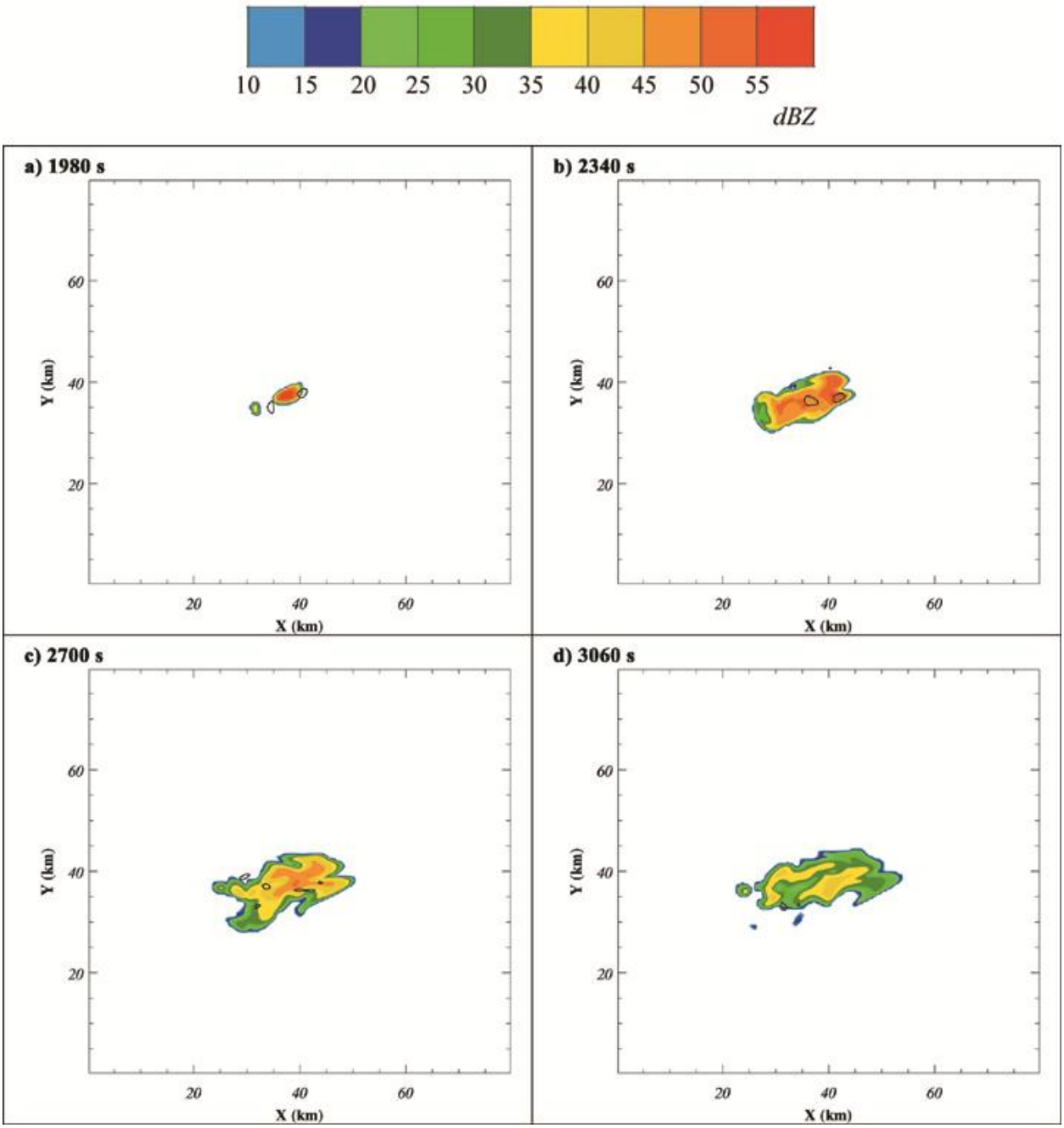

Figure 8: Surface simulated radar reflectivity (shaded, following the legend above) and vertical vorticity at 5 km AGL (contoured at 0.01 s^{-1} intervals; dashed contours indicate negative vorticity) for the warm-side simulation at a) 1980 s, b) 2340 s, c) 2700 s, and d) 3060 s.

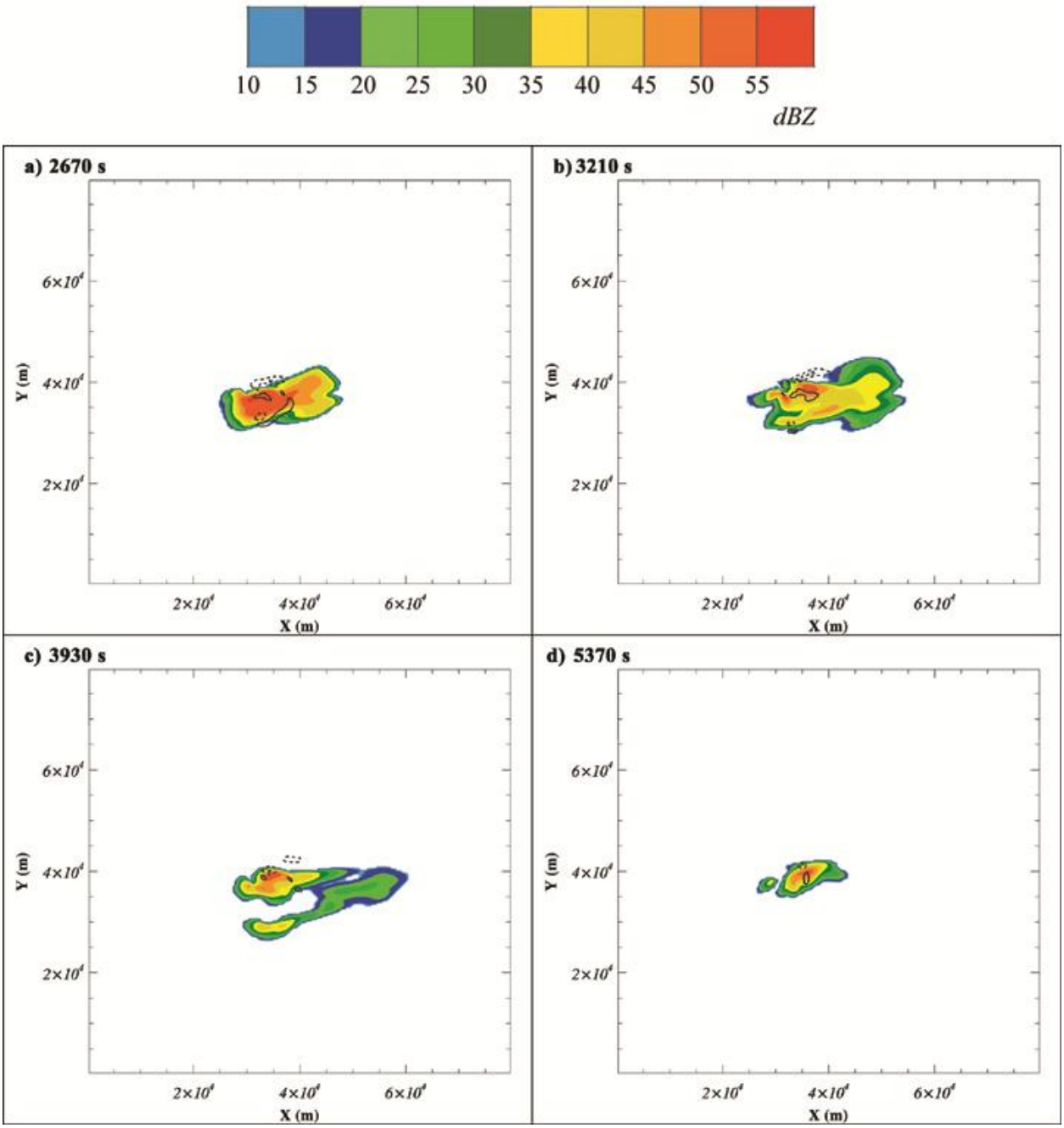

Figure 9: As in Fig.8, except for the cool-side simulation at a) 2670 s, b) 3210 s, c) 3930 s, and d) 5370 s.

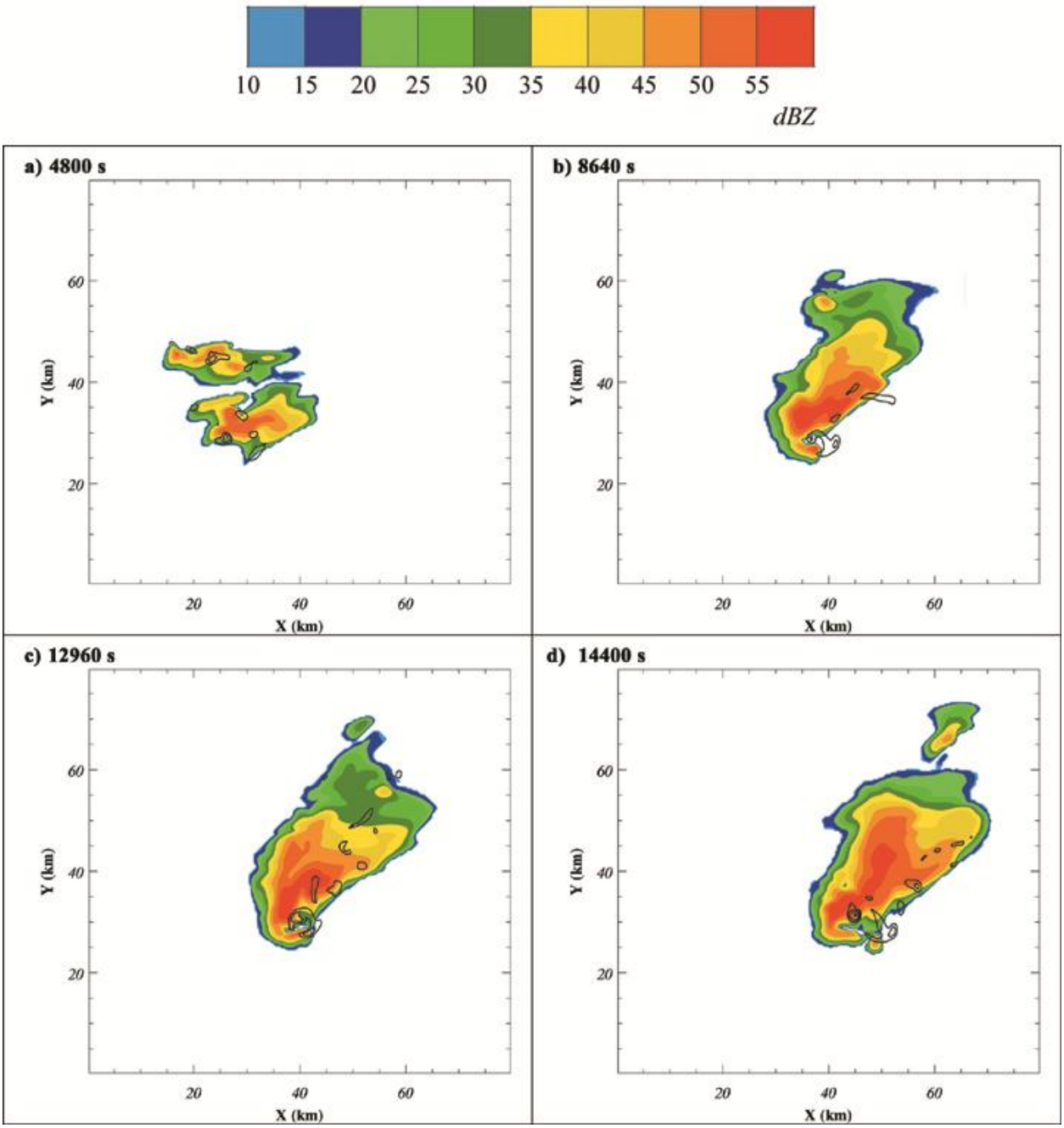

Figure 10: As in Fig. 8, except for the boundary simulation at a) 4800 s, b) 8640 s, c) 12 960 s, and d) 14 400 s.

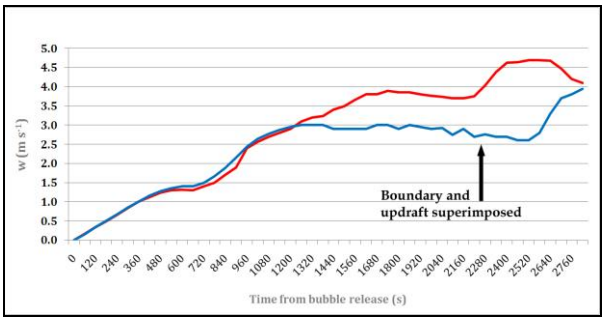

Figure 11: Time series of low-level (0.5 km AGL) vertical velocity for the updraft of the homogeneous warm-side storm (blue) and the boundary storm (red). *Click image to enlarge.*

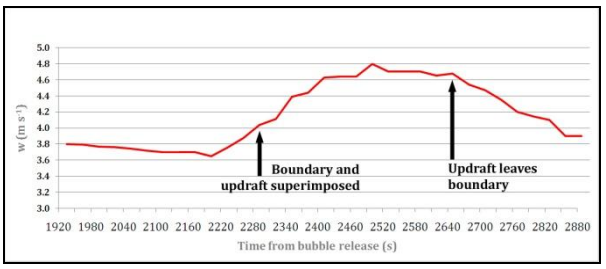

Figure 12: Time series of low-level (0.5 km AGL) vertical velocity for the updraft of the boundary storm, during boundary interaction. *Click image to enlarge.*

Vertical velocity decreased slightly before increasing again as the low-level updraft encountered the forced ascent (Figs. 11 and 12). As the storm continued to move to the east, the updraft became tilted at low-to-mid levels. The low-level updraft was still strongest along the area of forced ascent, but the midlevel updraft continued to shift southeast, and separated from the low-level updraft at ≈2400 s. Meanwhile, the low-level updraft, augmented by the forced ascent of the boundary, began expanding aloft and became evident at 5 km around 2760 s. This secondary updraft quickly became dominant, and the original low-level updraft dissipated completely by 3480 s. While this transition appeared as a decrease in the overall maximum vertical velocity from 2520–2880 s (Fig. 12), it actually marked the transition between dominant updrafts. Beyond this point, an overall increasing, then higher and relatively steady trend was seen in vertical velocity throughout the simulation (Fig. 7). Whether or not this was an indirect effect of the original direct augmentation of the vertical velocity, or merely that the second updraft developed in a more favorable location relative to the precipitation, is beyond the scope of this study. However, the trend in vertical velocity at low levels implies that the initial increase in updraft strength and development of the second updraft were direct results of the boundary. After the storm moved away from the boundary, low-level vertical velocity decreased slightly, implying that forced ascent no longer was impacting the updraft directly. As the storm moved over the cooler air mass, direct augmentation of the vertical velocity from forced ascent became nominal, thus other effects most likely dominated any increases seen in updraft strength.

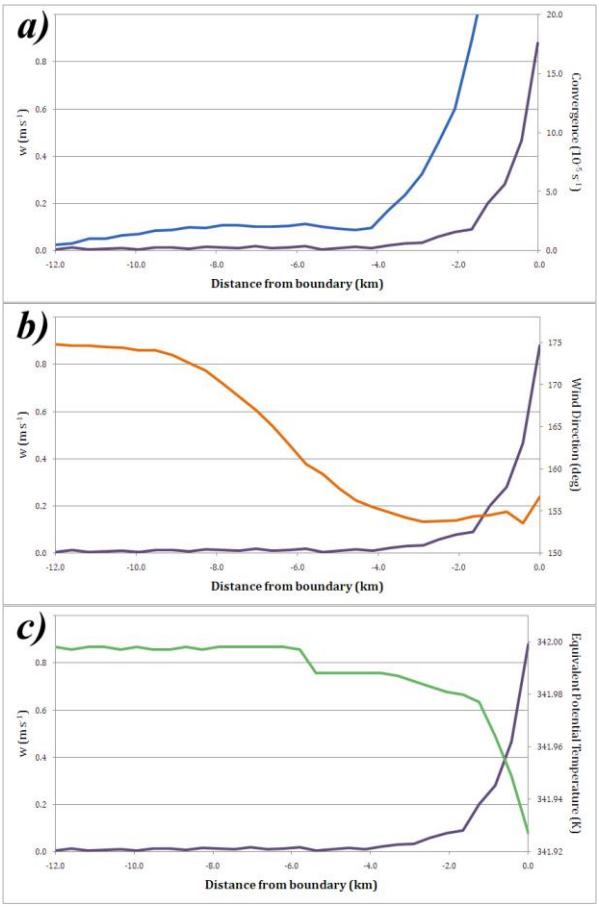

Figure 13: Plots of vertical wind speed (all panels; purple), with: a) convergence (blue), b) wind direction (orange), and c) θ_e (green), at decreasing distances from the boundary. *Click image to enlarge.*

b. Storm-splitting analysis

A major transition that occurred in the boundary storm was a split which began ≈30 min after precipitation reached the surface. This split was driven by a local deepening of the cool air mass by outflow from precipitation (Fig. 14a), which created forced

ascent similar to a gust front. A new updraft formed near the surface (~50 m AGL) at 3720 s and strengthened, splitting at mid levels around 4320 s. By 4800 s, this updraft had become stronger than the original. In the time series of vertical vorticity (Fig. 6), this period is characterized by lower overall maximum values in mesocyclone strength, before a sharp increase which began at 4920 s. This pattern relates well to the time series of maximum vertical velocity (Fig. 7), where overall updraft strength increased strongly beginning at 4800 s.

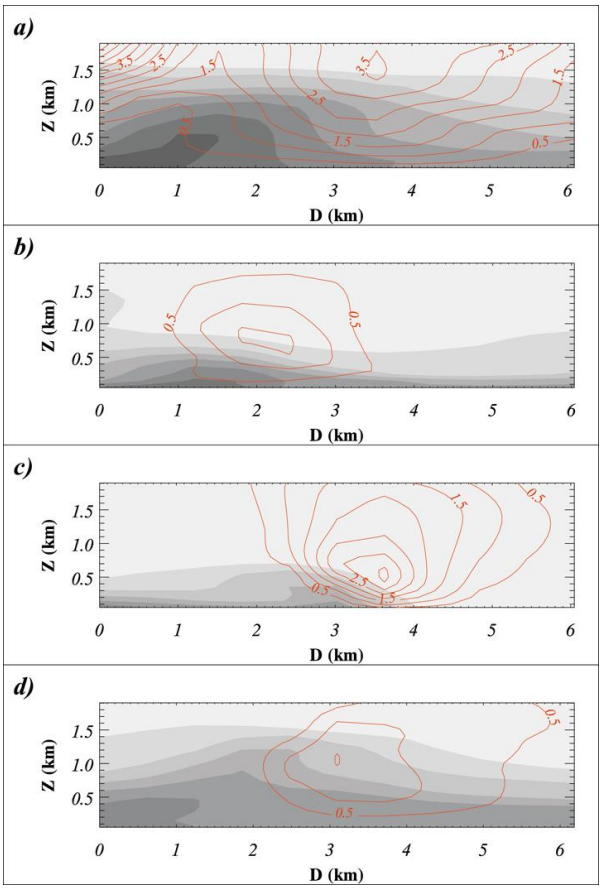

Figure 14: Cross section of virtual potential temperature (θ_v, shaded at 1 K intervals) and vertical velocity (red contours at 0.5 m s^{-1} intervals) through the strongest gust-front-induced low level updraft for a) the boundary simulation at 4200 s, b) the boundary simulation at 2400 s, c) the warm-side simulation at 2700 s, and d) the cool-side simulation at 3210 s. D indicates distance. The lightest gray represents θ_v of 312 K, with values decreasing thereafter. *Click image to enlarge.*

After the formation of the new updraft, the boundary storm moved more toward the southeast, and this updraft remained dominant throughout the remainder of the simulation. This change in motion was not the typical deviation that takes place when a storm becomes supercellular (Rotunno and Klemp 1982); the boundary storm contained a mesocyclone containing a negative pressure perturbation before the split. Instead, this change in storm motion was due to the development of the boundary storm's gust front. Before splitting, forced ascent along the storm's outflow was not strong enough to produce a low-level updraft (Fig. 14b). Once the vertical velocity produced by the combination of the cool air mass and gust front was strong enough to create a new updraft, splitting occurred, after which the air entering the main updraft was forced over the gust front. This induced a new storm motion and pulled the low-level updraft away from precipitation.

Splitting occurred and gust fronts were present in the homogeneous simulations (Figs. 14c and 14d); however, the strength of the combined gust front and cool air mass in the boundary simulation allowed the continual transitioning of the updraft away from precipitation that distinguishes the boundary storm from homogeneous storms. In homogeneous simulations, splitting occurred early and was driven by the shape of the hodograph (Bunkers et al. 2000) rather than by redevelopment along a gust front. In fact, the forced ascent along the gust fronts produced in the homogeneous simulations did not yield a low-level updraft that was strong enough to draw inflow continually from outside the region of precipitation. Figures 8–10 demonstrated that mesocyclones and mesoanticyclones in the homogeneous simulations quickly became immersed in precipitation, similar to the early behavior of the storm produced in the boundary simulation. The updrafts in the homogeneous simulations never were able to transition outside of precipitation, thus the storms were not able to persist. In contrast, the strength of the combined gust front and cool air mass in the boundary simulation allowed stronger forced ascent. The right-moving boundary storm therefore developed a new updraft outside the region of precipitation, subsequently split, and then continued to ingest warm, buoyant air.

The ability of the low-level updraft in the boundary storm to transition away from precipitation appears as a cyclic pattern in mesocyclone strength in the time series of maximum vertical vorticity (Fig. 6). Although the mesocyclone was largely steady state after splitting occurred, weakening and re-strengthening of the mesocyclone was observed throughout the remainder of the simulation. This pattern can be related to transitions of the location of the low-level updraft relative to precipitation. As

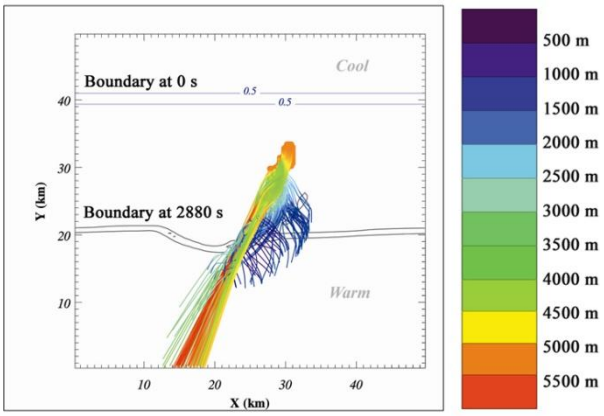

Figure 15: Boundary position at 0 s and 2880 s, and tracks of all trajectories terminating in the midlevel mesocyclone at 2880 s. Colors of the trajectories represent the height in the domain, following the legend on the right. *Click image to enlarge.*

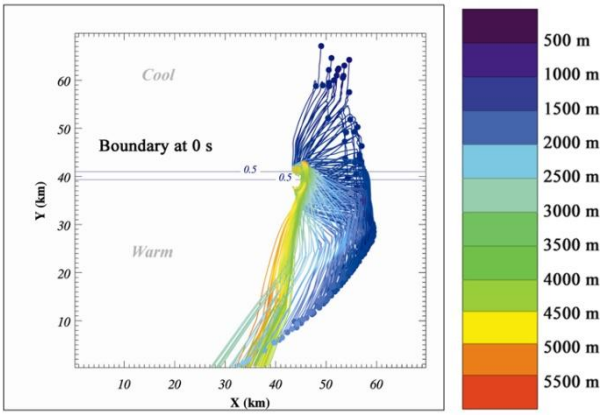

Figure 16: As in Fig. 15, except for 6000 s (boundary position at 6000 s located outside the domain). *Click image to enlarge.*

precipitation began falling in the low-level updraft, the response was an overall decrease in vertical vorticity. In contrast, as precipitation in the low-level updraft increased, outflow pushed farther away from the low-level updraft and began to translate away from precipitation, allowing the mesocyclone to strengthen. This transitioning behavior of the low-level updraft and cyclic behavior of the vertical vorticity is an important difference between the boundary storm and the storms produced in homogeneous simulations, and is apparent across a wide spectrum of analyses.

c. Trajectory analysis

As shown earlier, the boundary storm exhibited fundamentally different characteristics than the homogeneous storms. To examine the precise effect of the boundary on mesocyclone development, trajectories were calculated to examine the source of air parcels traveling into the mesocyclone and to determine how positive vertical vorticity in the mesocyclone was generated. Tracers were placed in the midlevel mesocyclone at multiple times and then were backwards-integrated to determine their source region. The midlevel mesocyclone was defined where vertical vorticity exceeded 0.01 s^{-1} at 5 km AGL, and tracers were placed in this vertical slice with a horizontal spacing of 200 m. Trajectory positions were calculated with a large time step of 120 s and a small time step of 30 s.

Early in the simulation (from 1920–3840 s), all tracers which terminated in the midlevel mesocyclone originated on the warm side of the boundary at multiple vertical levels (Fig. 15). These tracers were advected toward the mesocyclone by storm inflow and then were ingested by the updraft. As the storm moved farther over the cool side of the boundary, parcels terminating in the midlevel mesocyclone were drawn both from the warm and cool air masses (Fig. 16). Although some tracers originated on the warm side of the boundary, were lifted over the boundary, and then settled into the cooler air mass, the trajectories were split into two groups for the purpose of analysis: those originating from inside the cool air mass, and those originating and remaining in the warm side until ingestion in the mesocyclone. Although this procedure eliminated several trajectories from the analysis, it provided a better delineation between tracers that experienced enhancement from the boundary and those that did not. From 3840 s through the end of the simulation, there were at least two trajectories in each category, and the number of trajectories that originated in the cool air mass increased with time.

After dividing the trajectories into two groups, tracers were evaluated in two ways: a time series of vertical vorticity, and a time series of the contributions to the vertical-vorticity tendency. One representative tracer was selected from each group for each trajectory computation, in order to simplify the plots of the variables. For tracers that originated in either air mass, initial values of vertical vorticity were zero, since no preexisting vertical vorticity was present in the domain. As the updraft ingested the trajectories, vertical vorticity increased dramatically for those originating both in the warm and cool sides (Figs. 18 and 20). For tracers in the cool air mass, both stretching and tilting contributed positively to the vertical-vorticity tendency before the parcel was lifted into the mesocyclone. The

contribution from tilting then became negative as the parcel was lifted above the boundary (Fig. 17). In the warm air mass, tilting contributed positively to the vertical-vorticity tendency, while stretching contributed negatively (Fig. 19). The contribution from mixing, although plotted in Figs. 17 and 19, was negligible for both warm- and cool-side trajectories. In both the warm and cool sides of the boundary, initial vertical vorticity was generated via tilting of horizontal vorticity, after which vertical vorticity was available to be stretched and contribute to the vertical vorticity in the mesocyclone. Therefore, the tendency of vertical vorticity in tracers from both sides of the boundary primarily was due to tilting of horizontal vorticity.

In order to evaluate how parcels from each air mass contributed to the overall strength of the mesocyclone, the final value of vertical vorticity was analyzed for all trajectories that fell into one of the two groups. The largest values of vertical vorticity were from trajectories that originated and remained in the warm side until ingestion into the mesocyclone, while trajectories from the cool side of the boundary contributed only to the smallest values of vertical vorticity. This was consistent at all times for which trajectories were calculated, and can be seen in histograms that display the percentage of different vertical-vorticity ranges contributed by each group of trajectories (Fig. 21). Despite initially large amounts of horizontal vorticity available to be tilted into the mesocyclone, the cool-side tracers did not produce the largest values of vertical vorticity. This was due to a negative contribution from tilting which occurred as the tracers were lifted by the updraft, beginning at approximately 2.5 km AGL (Fig. 22). Although horizontal shear at this level still contributed to positive tilting (Fig. 23), a combination of both horizontal shear and horizontal gradients in vertical velocity determined the sign of the tilting term. As trajectories entered the mesocyclone from the north, a negative contribution to vertical vorticity from tilting was produced by increasing values of vertical velocity as the tracer moved southward (Fig. 24). This resulted in a lower ending value of vertical vorticity for trajectories originating in the cool side.

Trajectories terminating in the low-level (~1.5 km AGL) mesocyclone originated almost exclusively from the cool side of the boundary (Fig. 25). All trajectories, regardless of origination, traveled through the cooler air mass before being ingested into the mesocyclone, thereby experiencing horizontal vorticity enhancement. Due to the combination of the cool air mass and the gust front created by the storm itself, all warm air was force upward and did not enter the

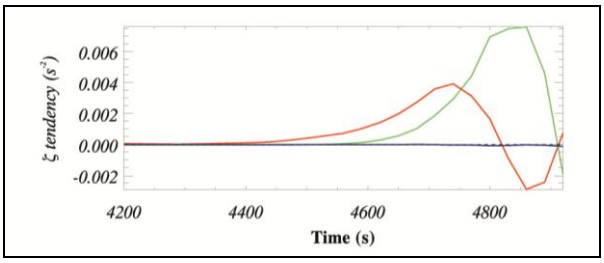

Figure 17: The contributions to vertical vorticity (ζ) from tilting (red), stretching (green), and mixing (blue) for a trajectory that represents tracers originating in the cool side of the boundary, scaled by a value of 10^2. *Click image to enlarge.*

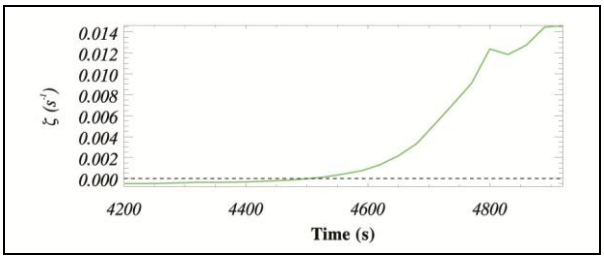

Figure 18: Vertical vorticity (ζ) for a trajectory that represents tracers originating in the cool side of the boundary. *Click image to enlarge.*

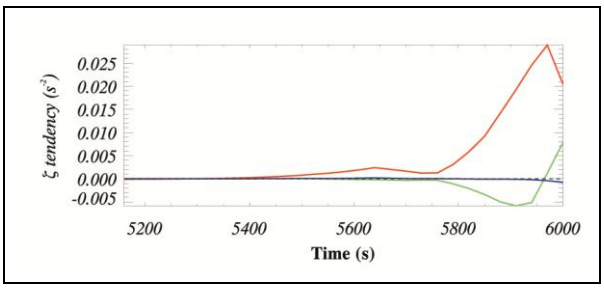

Figure 19: As in Fig. 17, except for the warm side. *Click image to enlarge.*

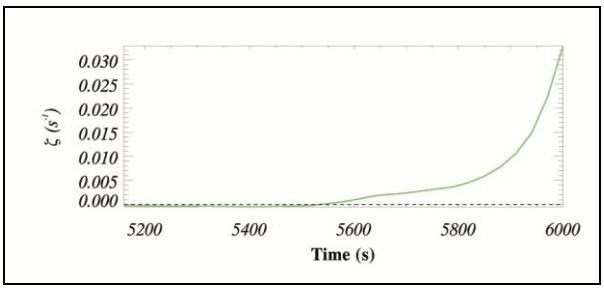

Figure 20: As in Fig. 18, except for the warm side. *Click image to enlarge.*

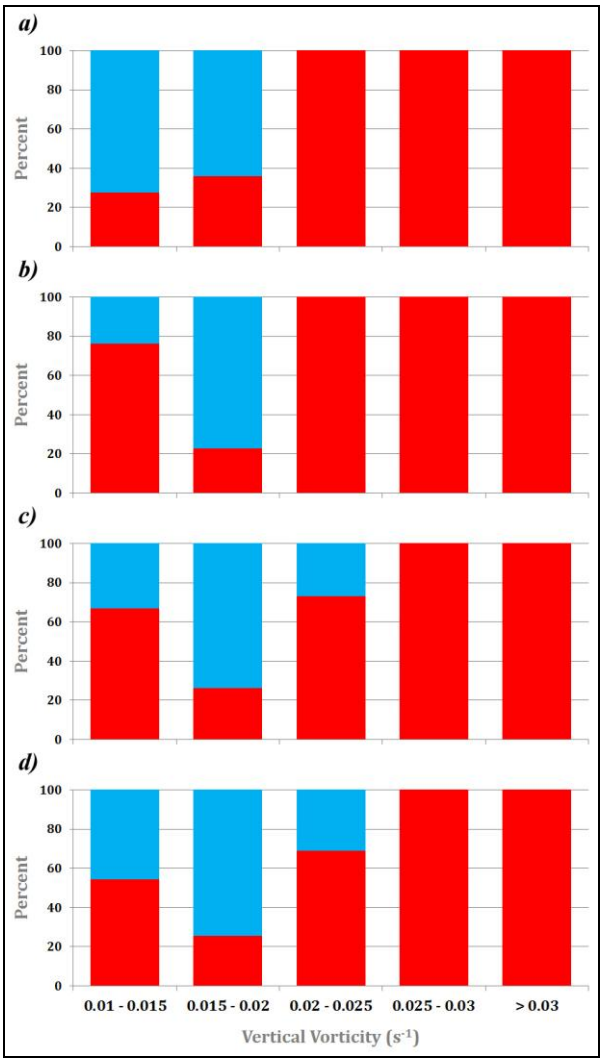

Figure 21: Histograms of the relative contribution from cool-side trajectories (blue) and warm-side trajectories (red) to vertical vorticity in the midlevel mesocyclone at a) 4920 s, b) 6000 s, c) 7680 s, and d) 9360 s. *Click image to enlarge.*

low-level updraft—thus the lack of contribution of tracers from the warm side to the vertical vorticity at cloud-base height. For trajectories entering the low-level mesocyclone, vertical vorticity was created primarily through stretching, which is reasonable in an area of forced ascent; however, tilting also contributed to positive vertical vorticity when the tendency initially became positive (Figs. 26 and 27).

After boundary interaction, the cloud-base height updraft had a maximum speed of ≈4 m s^{-1}; however, when the low-level mesocyclone formed, the vertical velocity at cloud base height was ≈9 m s^{-1}, which

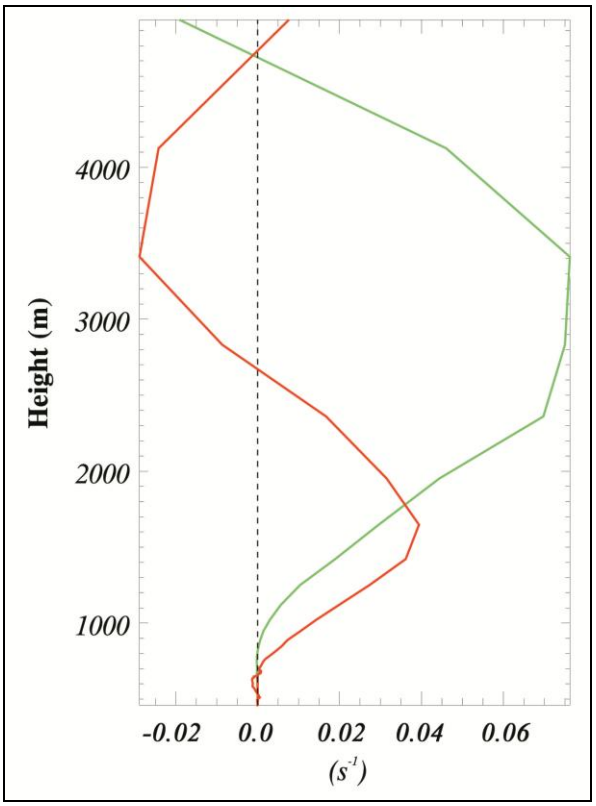

Figure 22: Vertical profile of the contributions to vertical vorticity (x-axis) from stretching (green) and tilting (red) for a trajectory representing tracers originating in the cool side of the boundary and terminating in the midlevel mesocyclone.

indicated a large enough contribution from stretching to obtain vertical vorticity exceeding 0.01 s^{-1} at low levels. As was discussed earlier, an increasing number of trajectories that terminated in the midlevel mesocyclone originated in the cool side as the storm progressed. This implies that the low-level mesocyclone was enhancing the main updraft, feeding back positively to the rotation at mid levels, and helping to support the longevity of the supercell.

By the time the boundary storm became relatively steady state, it was well over the cool-side air mass. Therefore, the homogeneous cool-side simulation would be expected to develop in a manner similar to the boundary storm. As was discovered in the time-series analysis, this was not the case. Although the homogeneous cool side contained a mesoanticyclone for a period of time, the right-splitting storm was not able to achieve the behavior of the persistent and steady-state mesocyclone found in the boundary storm. This most likely was due to the failure of the right-splitting component to develop into a supercell.

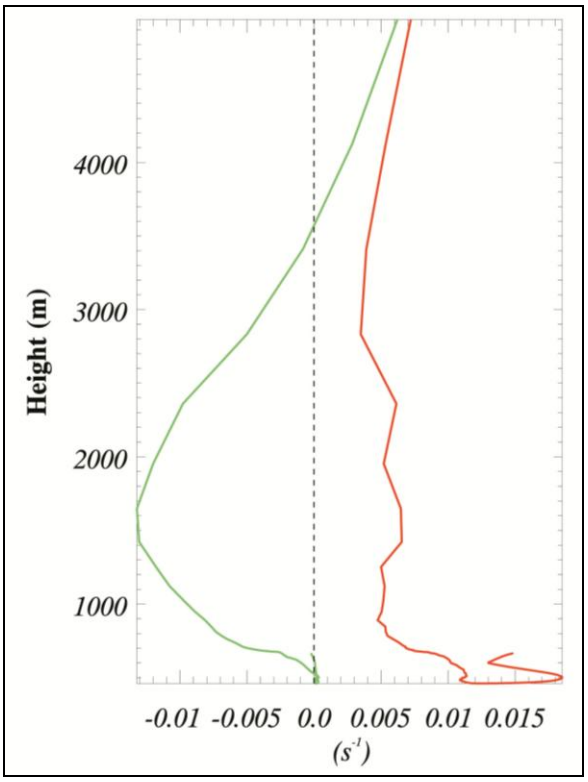

Figure 23: Vertical profile of vertical shear (s^{-1}) in the x-direction (green) and the y-direction (red) for a trajectory representing tracers originating in the cool side of the boundary and terminating in the midlevel mesocyclone.

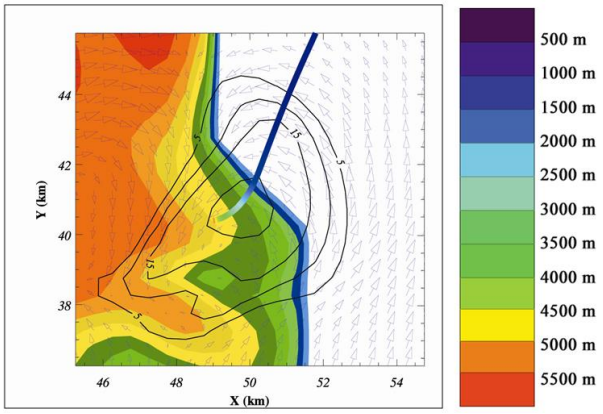

Figure 24: Trajectory representing tracers originating in the cool side of the boundary and terminating in the midlevel mesocyclone at 6840 s. Shading is reflectivity (as in Fig. 8), arrows are wind vectors at 3.5 km AGL, and contouring is vertical velocity at 3.5 km AGL, at 5 m s^{-1} intervals. Colors of the trajectory represent height in the domain, following the legend on the right. *Click image to enlarge.*

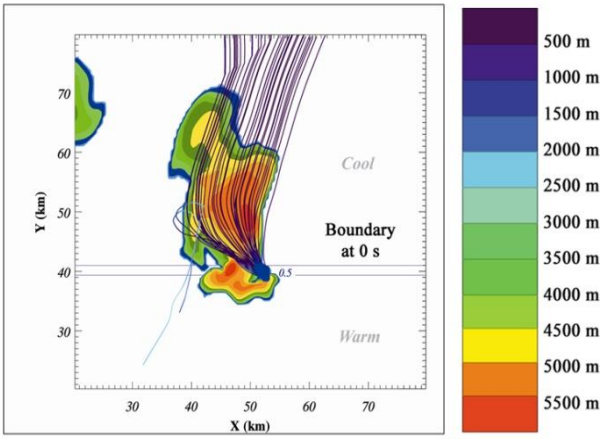

Figure 25: The position of the boundary at 0 s and the tracks of all trajectories terminating in the low-level (1.5 km AGL) mesocyclone for the boundary simulation at 7200 s. Shading is surface reflectivity at 7200 s (as in Fig. 8); colors of the trajectories represent height in the domain, following the legend on the right. *Click image to enlarge.*

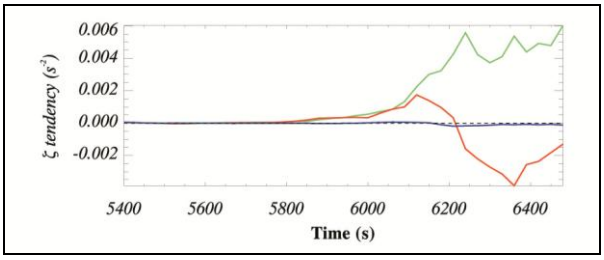

Figure 26: As in Figure 17, except for the low-level mesocyclone in the boundary storm. *Click image to enlarge.*

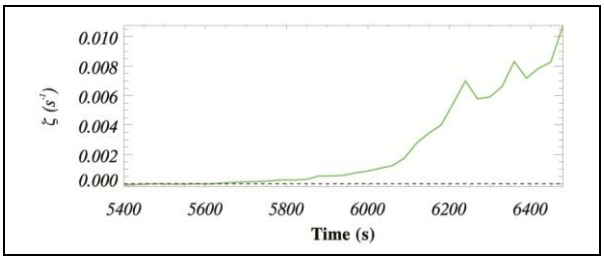

Figure 27: As in Fig. 18, except for the low-level mesocyclone in the boundary storm. *Click image to enlarge.*

Without augmentation of vertical velocity from an airmass boundary, the updraft on the right-splitting storm was very weak and dissipated quickly, as discussed in previous sections. Storm motion of the left-mover was to the north-northwest, which meant

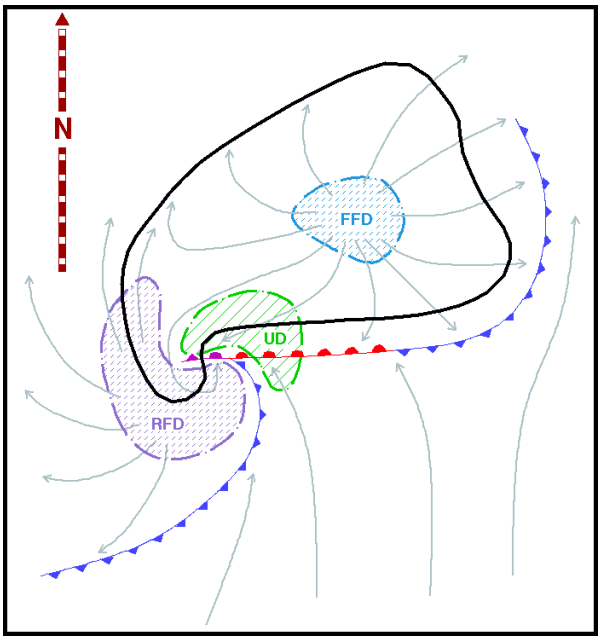

Figure 28: Schematic of a classic supercell, adapted from Lemon and Doswell (1979) by R. Edwards. FFD represents forward-flank downdraft; UD is the updraft, and RFD is the rear-flank downdraft.

precipitation was not moving in the same direction as the gust front; therefore, it could not maintain the strength seen in the boundary storm. Without the support of strong forced ascent from a combination of the gust front and cooler air mass, the updraft was not able to pull in air continually away from falling precipitation. As a result, the updraft became embedded in precipitation as the gust front weakened, and the storm was not able to persist.

4. Conclusions and summary

Overall, the boundary storm was stronger, longer-lived, and much more classic (similar to Fig. 28) in appearance than the other storms which were produced. The storms generated in homogeneous environments had maximum vertical-vorticity magnitudes of ≈0.03 s^{-1}, while the boundary storm more than doubled this amount after the mesocyclone became largely steady-state. The boundary storm was also much longer-lived than either of the homogeneous environment storms. It is clear that the boundary simulation produced a much more prototypical supercell than any of the homogeneous simulations, despite having the same CAPE and environmental shear as the original warm-side simulation. The presence of the boundary impacted the supercell in three ways: 1) forced ascent enhanced the updraft and allowed a stronger right-splitting storm to develop; 2) the stable layer on the cool side of the boundary combined with storm outflow to produce forced ascent which allowed the storm to transition away from precipitation and to continually draw non precipitation-cooled air; and 3) enhanced horizontal vorticity on the cool side of the boundary was readily available to be ingested into the low-level updraft, supporting the development and maintenance of a low-level mesocyclone.

The storm produced in the boundary simulation moved away from the boundary, but still experienced a comparative enhancement of mesocyclone strength and updraft strength throughout its life cycle. This implies that the boundary had an impact on the storm beyond the time that the storm was crossing the boundary and directly experiencing forced ascent. In fact, two of the previously discussed impacts of the boundary on the storm relate to the presence of the cooler air mass and not the boundary itself. However, the boundary simulation differed from both of the homogeneous simulations. It is the combination of both direct storm interaction with the boundary and the presence of the cooler air mass that produced a typically structured and long-lived supercell.

The presence of a preexisting airmass boundary had a dominant effect on the strength and longevity of the storm produced in the boundary simulation. Forced ascent from the airmass boundary created a stronger right-splitting storm that was able to persist long enough for a gust front to form and for the second split to occur. Once the storm moved over the cool side, the gust front and cool air mass combined to create forced ascent, promoting a long-lived supercell by allowing continual ingestion of warm air. In addition, enhanced horizontal vorticity from within the cooler air mass was continually ingested into the low-level updraft, which supported the presence and longevity of a low-level mesocyclone. Trajectories originating in the cool side were found at multiple levels in the mesocyclone, supporting a common assumption that the tilting of horizontal vorticity found in the denser side of an airmass boundary is important in supercell development (Markowski et al. 1998; Atkins et al. 1999; Rasmussen et al. 2000; etc.). In addition, the presence of the low-level mesocyclone appeared to be entirely a result of the horizontal vorticity enhancement found in the cool air mass, which is consistent with the results of Atkins et al. (1999). Although the results of this study are specific to one case, the common observance of supercell thunderstorms along airmass boundaries helps to support the application of these results to multiple cases and environments.

In operational meteorology, significant emphasis is placed on storms that develop along and interact with airmass boundaries. This study supports these findings and also emphasizes the lasting effects of an airmass boundary on mesocyclone longevity and strength. The results support continued operational emphasis on the recognition of airmass boundaries and their potential to impact a warning decision making situation. In addition, this study opens the door for further research into the role of an airmass boundary on midlevel mesocyclogenesis, particularly in nonsupercellular environments. Future work could include modeling additional cases in which a supercell forms along an airmass boundary in a nonsupercellular environment, in order to judge the sensitivity of the midlevel mesocyclone to the warm-side environment. Sensitivity tests of different vertical shear values or temperature perturbations in the airmass boundary also could be performed to see how the behavior of the mesocyclone changes and whether or not the supercell can become dominant with differing amounts of forcing from the airmass boundary. In addition, a follow-up study could expand on the role of forced ascent along the boundary in both low-level and midlevel mesocyclone strength. In summary, this study not only provides new insight into the role of airmass boundaries in supercell development, but also encourages further study into related topics.

ACKNOWLEDGMENTS

The authors would like to thank Jerry Straka (Univ. of Oklahoma), Matthew Bunkers (NWS Rapid City), Mark Conder (NWS Lubbock), and Robert Maddox for reviewing this article, as well as Philip Schumacher (NWS Sioux Falls), Scott Blair (NWS Topeka), Mark Anderson, (Univ. of Nebraska), Clinton Rowe (Univ. of Nebraska), Jeff Manion (NWS CRH), Roger Edwards (SPC), and Ryan McCammon (State of Wyoming) for technical editing. Additionally, we thank the University of Nebraska-Lincoln Department of Earth and Atmospheric Sciences and the University of Nebraska Layman Award for providing funding to support this work, as well as the Research Computing Facility (RCF) at the University of Nebraska-Lincoln for technical support and computing resources.

REFERENCES

Adlerman, E. J., K. K. Droegemeier, and R. P. Davies-Jones, 1999: A numerical simulation of cyclic mesocyclogenesis. *J. Atmos. Sci.*, **56**, 2045–2069.

Atkins, N. T., M. L. Weisman, and L. J. Wicker, 1999: The influence of preexisting boundaries on supercell evolution. *Mon. Wea. Rev.*, **127**, 2910–2927.

Browning, K. A., 1964: Airflow and precipitation trajectories within severe local storms which travel to the right of the winds. *J. Atmos. Sci*., **21**, 634–639.

Bryan, G. H., J. C. Wyngaard, and J. M. Fritsch, 2003: Resolution requirements for the simulation of deep moist convection. *Mon. Wea. Rev.*, **131**, 2394–2416.

Bunkers, M. J., B. A. Klimowski, J. W. Zeitler, R. L. Thompson, and M. L. Weisman, 2000: Predicting supercell motion using a new hodograph technique. *Wea. Forecasting*, **15**, 61–79.

Davies, J. M., 1993: Wind and instability parameters associated with supercell and non-supercell tornado events in the southern high plains. Preprints, *17th Conf. on Severe Local Storms*, St. Louis, MO, Amer. Meteor. Soc., 51–55.

Davies-Jones, R. P., 1984: Streamwise vorticity: The origin of updraft rotation in supercell storms. *J. Atmos. Sci*, **41**, 2991–3006.

Dostalek, J. F., J. F. Weaver, and G. L. Phillips, 2004: Aspects of a left-moving tornadic thunderstorm of 25 May 1999. *Wea. Forecasting*, **19**, 614–626.

Doswell, C. A. III, 2001: Severe convective storms—An overview. *Severe Convective Storms, Meteor. Monogr.* No. 28, Amer. Meteor. Soc., 1–26.

Gilmore, M. S., J. M. Straka, and E. N. Rasmussen, 2004: Precipitation evolution sensitivity in simulated deep convective storms: Comparisons between liquid-only and simple ice and liquid phase microphysics. *Mon. Wea. Rev.*, **132**, 1897–1916.

Hart, J. A., and W. Korotky, 1991: The SHARP workstation v1.50 users guide. National Weather Service, NOAA, 30 pp. [Available from NWS Eastern Region Headquarters, Scientific Services Division, 630 Johnson Ave., Bohemia, NY 11716.]

Houston, A. L., 2004: The role of preexisting airmass boundaries in the maintenance and rotation of deep convection in a high-CAPE, low-shear environment. Ph.D. thesis, Dept. of Atmospheric Sciences, University of Illinois at Urbana-Champaign, 275 pp. Available from the Univ. of Illinois Library, 1408 W. Gregory Dr., Urbana, IL 61801.

——, and D. Niyogi, 2007: The sensitivity of convective initiation to the lapse rate of the active cloud-bearing layer. *Mon. Wea. Rev.*, **135**, 3013–3032.

——, R. L. Thompson, and R. Edwards, 2008: The optimal bulk wind differential depth and the utility of the upper-tropospheric storm-relative flow for forecasting supercells. *Wea. Forecasting*, **23**, 825–837.

Klemp, J. B., and R. Wilhelmson, 1978: The simulation of three-dimensional convective storm dynamics. *J. Atmos. Sci*, **35**, 1070–1096.

Lemon, L. R., and C. A. Doswell III, 1979: Severe thunderstorm evolution and mesocyclone structure as related to tornadogenesis. *Mon. Wea. Rev.*, **107**, 1184–1197.

Maddox, R. A., L. R. Hoxit, and C. F. Chappell, 1980: A study of tornadic thunderstorm interactions with thermal boundaries. *Mon. Wea. Rev.*, **108**, 322–336.

Markowski, P. M., E. N. Rasmussen, and J. M. Straka, 1998: The occurrence of tornadoes in supercells interacting with boundaries during VORTEX-95. *Wea. Forecasting*, **13**, 852–859.

Mesinger, F., and Coauthors, 2006: North American regional reanalysis. *Bull. Amer. Meteor. Soc.*, **87**, 343–360.

Moller, A. R., C. A. Doswell III, M. P. Foster, and G. R. Woodall, 1994: The operational recognition of supercell thunderstorm environments and storm structures. *Wea. Forecasting*, **9**, 327–347.

Rasmussen, E. N., and D. O. Blanchard, 1998: A baseline climatology of sounding-derived supercell and tornado forecast parameters. *Wea. Forecasting*, **13**, 1148–1164.

——, S. Richardson, J. M. Straka, P. M. Markowski, and D. O. Blanchard, 2000: The association of significant tornadoes with a baroclinic boundary on 2 June 1995. *Mon. Wea. Rev.*, **128**, 174–191.

Rotunno, R. and J. B. Klemp, 1982: The influence of the shear-induced pressure gradient on thunderstorm motion. *Mon. Wea. Rev.*, **110**, 136–151.

Schlesinger, R. E., 1975: A three-dimensional numerical model of an isolated deep convective cloud: Preliminary results. *J. Atmos. Sci.*, **32**, 934–957.

Smith, P. L. J., C. G. Myers, and H. D. Orville, 1975: Radar reflectivity factor calculations in numerical cloud models using bulk parameterization of precipitation. *J. Appl. Meteor.*, **14**, 1156–1165.

Thompson, R. L., R. Edwards, J. A. Hart, K. L. Elmore, and P. M. Markowski, 2003: Close proximity soundings within supercell environments obtained from the Rapid Update Cycle. *Wea. Forecasting*, **18**, 1243–1961.

Weisman, M. L., and J. B. Klemp, 1982: The dependence of numerically simulated convective storms on vertical wind shear and buoyancy. *Mon. Wea. Rev.*, **110**, 504–520.

Wicker, L. J., and R. B. Wilhelmson, 1995: Simulation and analysis of tornado development and decay within a three-dimensional supercell thunderstorm. *J. Atmos. Sci.*, **52**, 2675–2703.

Ziegler, C. L., and E. N. Rasmussen, 1998: The initiation of moist convection at the dryline: Forecasting issues from a case study perspective. *Wea. Forecasting*, **13**, 1106–1131.

REVIEWER COMMENTS

[Authors' responses in *blue italics.*]

REVIEWER A (Jerry M. Straka):

Initial Review:

Recommendation: Revisions required.

Major Comments: The Introduction is well written and quite complete.

In section 2 the SCP may not be well known except to a few familiar with where to find a definition. I would suggest a) stating what it stands for and b) how to compute it. Alternatively you could a) state what it stands for and b) reference where on the Storm Prediction Center where to find this.

When the SCP is first introduced in section 1, an expansion of the abbreviation and a reference to Thompson et al. 2003 were included for explanation of the parameter. The authors have also added a link to the Storm Prediction Center website to supplement the reference.

I was disgruntled a bit at making comparisons of simulations with different initiation mechanisms on the various sides of the boundary and on the boundary. I would have used a prescribed thin spheroidal vertical velocity field, computed dw/dz, set –del dot V_h = -delta = to dw/dz (or use the anelastic equation) for more completeness, and the solved for the u and v fields from the kinematic relationships found in Bluestein (1992; pg, 87) where u = ½ * delta * x, and v = ½ * delta * y. I have found this to be a very effective convective mechanism, especially for stable boundary layers. Alternatively, what happens when you try to simulate a supercell on the boundary and in the homogeneous warm air with an elevated bubble? As it is you have too many things varied in the model to make fair comparisons.

The homogeneous cool side simulation was originally run with a surface-based warm bubble to maintain consistency among simulations (not shown in the paper); however, due to the presence of the stable layer at the surface, deep convection was not sustainable with surface-based initiation. The elevated bubble release was meant to more realistically represent how a parcel would be lifted above a stable layer, while the surface-based bubble released in the warm and boundary simulations were meant to represent convective initiation in a well-mixed environment. The authors believe that using identical initiation mechanisms would result in simulations that should not be compared, as it may be unrealistic to assume that parcels are lifted in an identical manner on both sides of an airmass boundary.

Also, on Fig. 3, can you plot vertical vorticity and one with moisture convergence to compare with the studies by Maddox? Does your outflow produce convergence that can be compared to the NARR data (you will have to sample it model data by filtering it).

Figure 3 has been split into two figures, one which is the original Figure 3 (now 3a) and a new figure with moisture convergence and vertical vorticity (3b). However, if the model output was filtered to a 32-km grid as in the NARR output, too few gridpoints would be available to compute vorticity, so a direct comparison of the model-produced airmass boundary and the outflow boundary in the case study is not possible. Additionally, a comparison of vorticity from the model output and the NARR data may not be an appropriate illustration, as the model output is intended to represent but not replicate the case study, due to the idealized nature of the model simulations.

The domain seems rather small (only 80 km on a side), and the horizontal grid resolution rather large for work these days (500m). I think, based on studies of convection by many many others, one should stay on the smaller side or equal to 250 m grid spacing in the horizontal (Bryan, personal communication). Also since low-level features are key in this study, more resolution in the boundary layer might be needed?

The domain was translated to follow the motion of the simulated storm, which decreased the domain size necessary for simulations, and there was not an issue of the main supercell storm reaching the edge of the domain in any of the simulations. The grid spacing used (500 m) is similar to or smaller than the grid spacing used in several recently published papers that capture similar phenomena (Frame and Markowski 2010; Ziegler et al. 2010; Morrison and Milbrandt 2011; Nowotarski et al. 2011). In addition, the vertical spacing of the boundary layer was prescribed to be as small as possible without creating unrealistic "pancake" grid boxes through the low-levels of the domain. With the computational resources available, the authors feel that the grid spacing and domain size were reasonable to resolve the features discussed in this paper. The authors have acknowledged the work of Bryan et al. (2003) in the text of the paper.

Frame, J., and P. Markowski, 2010: Numerical simulations of radiative cooling beneath the anvils of supercell thunderstorms. Mon. Wea. Rev., ***138**, 3024–3047.*

Ziegler, C. L., E. R. Mansell, J. M. Straka, D. R. MacGorman, and D. W. Burgess, 2010: The impact of spatial variations of low-level stability on the life cycle of a simulated supercell storm. Mon. Wea. Rev., ***138**, 1738–1766.*

Morrison, H., and J. Milbrandt, 2011: Comparison of two-moment bulk microphysics schemes in idealized supercell thunderstorm simulations. Mon. Wea. Rev., ***139**, 1103–1130.*

Nowotarski, C. J., P. M. Markowski, and Y. P. Richardson, 2011: The characteristics of numerically simulated supercell storms situated over statically stable boundary layers. Mon. Wea. Rev., ***139**, 3139–3162.*

[Editor's Note: The Nowotarski et al. reference was in press at the time of the review; specific publication information since has been added.]

Was surface friction included in the simulations?

No, surface friction was not included due to the idealized nature of the simulations.

[Minor comments omitted...]

Second review:

Recommendation: Revisions required.

General Comments: The authors have addressed many of the reviewer's questions, though several issues stand out, which are real game players in determining whether the paper should be published or not in my opinion. I acknowledge the significant amount of work the authors have done, but all possibilities need to be considered regarding the issues briefed below before publishing.

I spent perhaps three hours or more to review all the Lubbock 88D radar data in 2D and 3D using IDV and 2-D with the NOAA Tool Kit around storm initialization and development times. I did this based on Bunkers' finding of where the storm seems to be relative to the boundary placement—that is on the cool side of the boundary. It is very difficult given the storm distance from the radar to say where exactly where the base of the storm is early on its development. Moreover, the storms first echo forms aloft, and likely well over the cool side of the boundary, further leaving much doubt as to where the base of the storms actually might have been. By the way, I looked for the Amarillo and Clovis radar 88D data but only Lubbock was available on 25 May 1999. The Clovis data would have been particularly useful for this case.

There seems as if there was not a very careful enough comparison of NARR data, which has several problems (such as boundary placement and super adiabatic layers near the lower boundary so I recently learned), with actual data to more carefully place the boundary. Note that the NARR data uses the hybrid step/sigma-p coordinate system. Placement of the boundary using a ≈30 km resolution data set that was

developed with a model that does not explicitly resolve convection makes the boundary position in the data, within ≈30 to ≈90 km of its actual location, probably dubious if I do indeed understand the NARR data set development based on the Mesinger et al. (2006 BAMS) article.

As it stands, I think this is a nice stand alone boundary crossing simulation with the warm side initialization attempts (then why bother with a cool side initialization attempt?). Unfortunately, because of the difficulty of placement of the actual initial storm, the verisimilitude attempt gets the authors in trouble and essentially ruins the paper in my honest opinion—the actual storm may have formed on the cool side of the boundary as pointed out by Bunkers and my further analysis. Or it may have formed right on the boundary. If either of these is actually the case then Bunkers arguments and my further analysis would make the paper difficult to accept as a boundary/supercell interaction/crossing paper. Finally if the storm actually formed on the convergence boundary, this would further support my initial contention of using a lower-level convergence initialization approach rather than bubble initialization approach to initiate storms.

In the end I would say the authors have three options. They could a) withdrawal the paper, b) they could recast the paper as an idealized boundary crossing/interaction paper without the cool side initialization attempt and without the verisimilitude, or c) skip the warm side initialization attempts and investigate initialization of storms on boundaries or cool sides of boundaries.

This paper has been a very difficult one to review. Like I initially wrote in this review I acknowledge the hard work done to produce the paper. But there are too many 'ifs' in the paper to accept it in its present form. My recommendation is to give the authors the chance to reconsider how the paper is cast, which still would be a very significant major revision as I recommended initially in my first review.

The authors feel that the portion of Section 2 which described the case study environment and storm development confused the overarching purpose of the manuscript. It was not intended that the simulations would mirror the case study, which is an unrealistic assumption due to the idealized nature of model. Instead, the purpose of the case study was simply to initialize the model with an environment in which supercell development was observed in proximity to a preexisting outflow boundary. To avoid the comparison of simulated storms with the case-study storms by readers, this portion of Section 2 has been removed.

Regarding the homogeneous cool side simulation, the authors have opted to retain this segment of the paper for the sake of comparison with the boundary simulation. Due to the boundary storm's movement over the cool side for the majority of the simulation, it can be questioned whether the airmass boundary or the cool air mass itself is influencing storm mode. For this question to be answered, the cool side simulation is necessary.

REVIEWER B (Matthew J. Bunkers):

Initial Review:

Reviewer recommendation: Accept with major revisions.

General comments:

This is an interesting paper that has noteworthy application to severe storms forecasting. To my knowledge, there hasn't been any work done like this before. The study highlights some of the potential impacts of boundaries on supercellular development, and appears to support anecdotal observations.

I have mostly minor comments, but do have enough major comments that I would like to see the paper for a second review. I also faced several deadlines, and therefore wasn't able to give the paper the kind of review that I would have liked.

All of my suggested changes are contained in the annotated manuscript; please refer to that for full details. On the next page begins a listing of my comments that also are contained in the annotated manuscript.

EJSSM scientific content checklist:

1. References in support of an assertion – good
2. Speculation – kept at a minimum
3. Significance of results – you only have one case study (which was noted), but your paper still has general applicability
4. Reproducibility – methods are well described
5. Proof – the implied hypothesis (an airmass boundary can assist in supercell development) generally is well supported; but midlevel dry air should be addressed
6. Relevance – very good
7. Originality – very good
8. Comparisons with existing work – proper background information was provided, but I would like to see a mention of the relevance of the work of Loftus et al. (2008)
9. Negative results – N/A

EJSSM quality of presentation checklist:

1. Quality of figures – generally good, but some need larger font
2. Quality of the English – verb tense needs to be corrected through much of paper
3. Organization – good
4. Completeness – generally good, but a few citations/references need fixing

Major comments:

1. Models have struggled to produce convection in relatively dry midlevel environments (see Bunkers 2010). Thus, I would like to know if you ran simulations with RH set to 90% as done in McCaul et al. (2005), among others. I believe this topic needs to be addressed to help confirm the validity of your results (i.e., run warm and cool simulations with RH = 90%). Moreover, I believe you need to refer to Loftus et al. (2008) because that study has implications for your work. Specifically, they weren't able to get sustained convection with an initiating bubble, but they did get sustained convection when the flux techniques were used for initiation. This is not the same as what you did, but their momentum flux technique represented a boundary, so you should state how that relates to your work.

Bunkers, M. J., 2010: How midlevel horizontal humidity gradients affect simulated storm morphology. Preprints, *25th Conf. on Severe Local Storms*, Denver, CO, Amer. Meteor. Soc., P7.1.

Loftus, A. M., D. B. Weber, and C. A. Doswell III, 2008: Parameterized mesoscale forcing mechanisms for initiating numerically simulated isolated multicellular convection. *Mon. Wea. Rev.*, **136**, 2408–2421.

McCaul, E. W. Jr., C. Cohen, and C. Kirkpatrick, 2005: The sensitivity of simulated storm structure, intensity, and precipitation efficiency to environmental temperature. *Mon. Wea. Rev.*, **133**, 3015–3057.

To address the concern that midlevel dry air was affecting the development of storms in the homogeneous simulations, both the warm and cool side simulations were re-run with 90% relative humidity above the LCL. Although surface precipitation was much more abundant, a coherent, long lived supercell failed to develop in either of the simulations. This suggests that while midlevel dryness was a large factor in the amount of precipitation produced by the simulated storms, it did not improve the storms' ability to become organized. In this study, the ability of the main rotating updraft to transition outside of precipitation was paramount to obtaining a long-lived supercell–and with more precipitation falling, less midlevel dryness may actually inhibit these storms further from developing persistent updrafts.

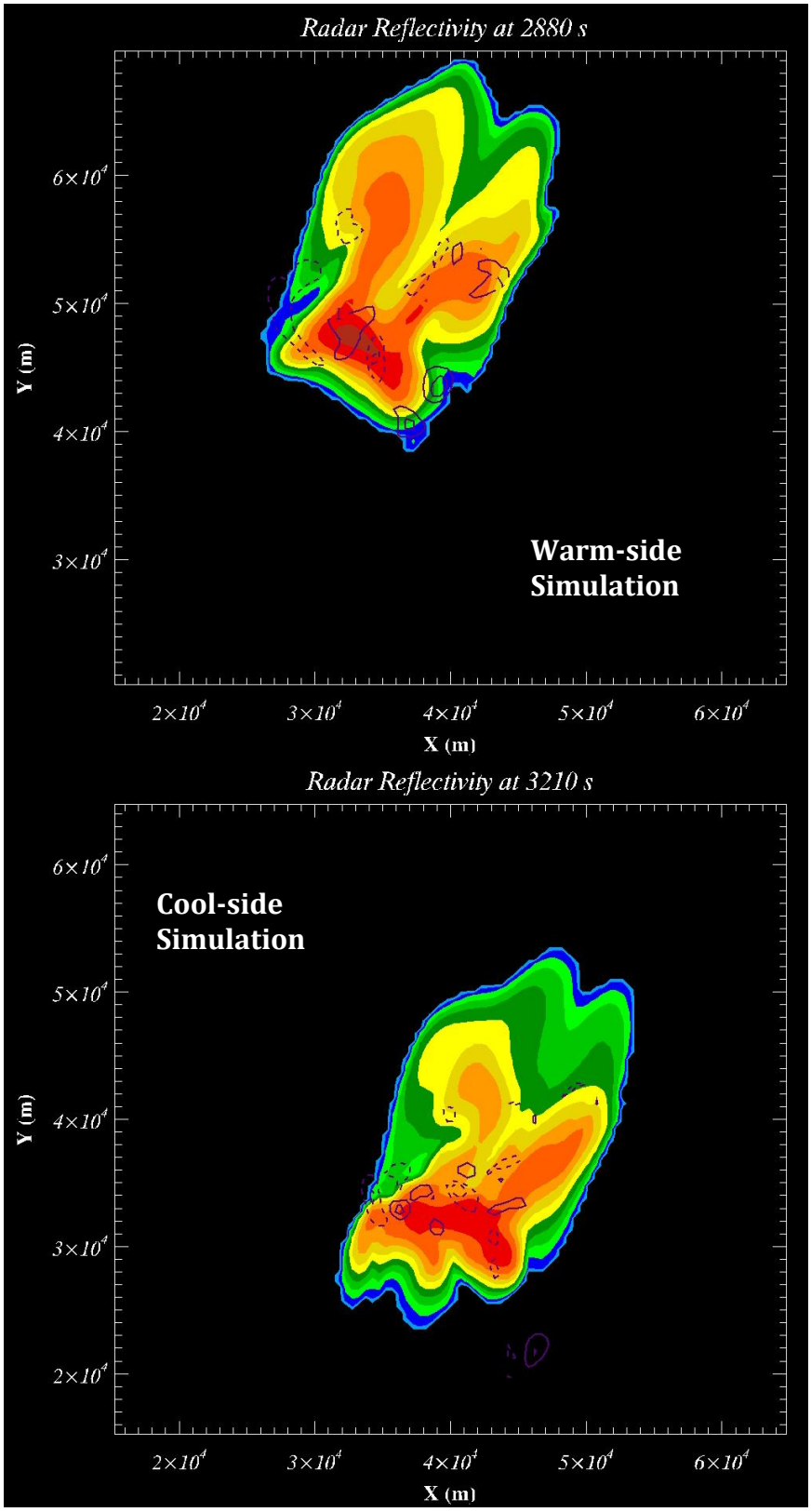

Regarding the work of Loftus et al. (2008), the authors could not find a relevant place to include this research within the manuscript, since Loftus et al (2008) primarily considers multicellular development

and is more interested in the initiation phase than the development of a mesocyclone. The study in consideration does make the point that storm initiation is rare in homogeneous environments (without an airmass boundary or other heterogeneity), and the results of the current study are in apparent agreement with this assessment.

2. One of my biggest concerns throughout the paper is with verb tense dominated by present form; I've never seen an AMS-published paper written in this way. Abstracts are the exception. It is standard to write about past studies in past tense (i.e., Maddox et al. suggested such-and-such back in 1980; they are not suggesting it now). The same goes for what you have already done (i.e., methods and results). Please check through all of your verb tense usage and ensure it is past tense when talking about things in the past or work that you have already done (e.g., the simulated supercell split after 30 min, etc.). I've tried to make the edits, but I likely have missed some.

The paper has been modified to correct the verb tense.

3. Regarding the vorticity values on p. 7, if you are comparing the mesoanticyclone to the mesocyclone, you need to specify **absolute** values because they are of the opposite sign. Also, use negative values for the vorticity when appropriate (e.g., first paragraph on p. 9 when you refer to the left mover). In addition, a left-moving supercell doesn't have mesocyclonic rotation; it has mesoanticyclonic rotation (in the Northern Hemisphere). There are several places in the paper where "mesocyclone" is used loosely for both right- and left-moving storms; please fix these.

The figures and values throughout the paper that address vorticity have been modified to indicate absolute values or magnitudes when appropriate (such as for comparison with positive, mesocyclonic values) and have been changed to negative values elsewhere. The terminology has also been corrected to indicate mesoanticyclonic rotation when vorticity is negative.

4. This might not appear to be major, but to make Figs. 8 and 9 more intuitive, I suggest the line colors are changed to cool = blue, warm = red, and boundary = green (for go, which is what the boundary made the supercell do). I find it counterintuitive to see the warm simulation labeled as blue; this was confusing when interpreting these two figures.

The colors have been modified to reflect the suggestion of the reviewer.

[Minor comments omitted...]

Second Review:

Reviewer recommendation: Accept with minor revisions.

General comments: I have finished my review. In my opinion the authors have done a fine job of revising the paper and have addressed my major concerns. I have several minor comments and some corrections in the attached MS Word document. Below I have listed my most notable concerns. I believe the paper is suitable for publication after these items are addressed.

1) Regarding Table 1 and the cool side environment, if you calculate SRH using the left-moving storm motion, then I suspect it would be much smaller than 107 $m^2 s^{-2}$ in your Table 1. In fact, it could very well be –107 $m^2 s^{-2}$. Please verify this value.

SRH of –107 $m^2 s^{-2}$ is correct, and this has been modified in the text.

2) Regarding the statement on p. 12 where storm splitting occurred 40 minutes after the bubble was released, this contradicts with Figs. 8 and 9 which indicate that splitting occurred 60–100 min after the bubble was released. Please clarify this.

The splitting annotated on Figs. 8 and 9 refers to the splitting of the right-moving storm described in Section 3b. The annotation has been modified for clarity to "R-mover Splitting."

3) On p. 13 you talk about a split that occurred 30 min after precipitation formed at the surface. Is this a second split, or is this the same split noted on the top of p. 12? If it is the same split, why the different times?

This is a different split (of the right-moving storm, after the right- and left-moving components are already separated) which is annotated in Figs. 8 and 9.

4) Regarding the bottom of p. 13, this seems to contradict what is stated immediately on the next page (i.e., Splitting occurred and gust fronts were present in the homogeneous simulations…"), because on p. 13 you imply that splitting can only occur after the cool air mass and gust front act synergistically. This cannot happen in the homogeneous simulations because there is no boundary. Please clarify.

The splitting described in the homogeneous storms is that which occurs in all simulations; the separation of the left- and right-moving components. In Section 3b, a more notable second split occurs in the right-mover, which is due to the combination of the cool air mass and gust front, not by the dynamics of rotation that drive initial splitting.

[Minor comments omitted...]

REVIEWER C (Mark R. Conder):

Initial Review:

Reviewer recommendation: Accept with major revisions.

Substantive comments (numbered notes):

#1: Use of the terminology, "airmass boundary" seems somewhat uncommon in the literature. Markowski et al. (1999) used the term "boundary" to refer to outflows, fronts, anvil-shading zones, etc. Instead of having to define "airmass boundary" on page 2, would it be preferable to just use "boundary" or possibly "baroclinic boundary" as the density difference is the primary identifying feature? Also, I can't find a definitive answer whether or not "air mass" or "airmass" is preferable. Not a big concern, I have no problem with "airmass boundary" remaining in the paper.

The authors have used the terms "airmass boundary" and "boundary" interchangeably throughout the paper. When the term is first defined, it is described as the demarcation between two air masses, and the term "airmass boundary" lends more specificity to this definition. Since both terms are meant to describe the same feature, the authors have opted to keep the terminology as originally written.

#2: My understanding is that the term "gust front" used in this paper primarily refers to the forward-flank gust front in the supercell. Does your model analysis suggest the presence of/interaction with the rear-flank downdraft (sometimes called rear-flank gust front)? I suspect that 500-m horizontal resolution might be on the low side to distinguish between the two features since the RFD is usually smaller. Do you think it would be helpful to mention the forward flank specifically in the discussion?

Throughout the paper, the term "gust front" refers to the forward-flank gust front. Since the primary impact of the gust front was to bring unadulterated inflow to the parent updraft, interactions of the rear-flank downdraft with the storm are generally not discussed. The terminology has been reworded so that the first mention of a "gust front" (on pg. 3) has now been changed to "forward-flank gust front (hereafter, gust front)."

#3: This sentence may be somewhat contradictory. If the synoptic-scale environment was generally (if weakly) supportive of supercell development as summarized in Table 1, why did it require a prominent boundary to generate a supercell ("necessary for supercell development")? I think the sentence might be better rephrased with a focus on "degree". Such as the ambient environment was not "optimally" supportive of supercells, or that the supercell had a stronger or more sustained mesocyclone than without the aid of a boundary.

This point is one of the primary conclusions of the paper—that despite an environment that generally supports supercell development, a boundary is still required to generate a long-lived supercell. Although it seems counterintuitive, it is similar to the findings of Markowski et al. (1998), which is discussed in the introduction.

#4: I'm not sure I understand the sounding methodology for the boundary simulation. Figures 5 and 6 show the warm and cool soundings from the homogeneous simulations. Am I correct in interpreting that you used the warm-side NARR sounding to initialize the entire domain for the boundary simulation, but then you added the shallow cool air across the northern part—so the boundary layer simulation is the same as the warm homogenous, except for the shallow cool layer in the northern portion of the domain? Does the outflow boundary portion in the boundary simulation have the same low-level wind profile as the cool homogeneous simulation?

The entire domain is initialized with the NARR warm-side sounding, then the shallow cool airmass is added to half of the domain. The cool side homogeneous simulation is initialized with a sounding taken from the boundary simulation (in the cool side); therefore, the cool side simulation has the same low-level wind profile as the outflow boundary in the boundary simulation. A cool side NARR sounding was only taken to best prescribe the characteristics of the outflow boundary, but was not used to initialize any of the simulations. The caption for Figure 6 has been modified for clarity.

#5: The actual storm evolved into a HP supercell, were there any indications of this in the model precip/reflectivity fields in the boundary simulation or can you speculate what environmental differences there might have been? Or to put it another way, are you satisfied that the low-level moisture was adequately represented? Taking a look at the 18 UTC sounding from KAMA in Dostalek 2004, the low-level moisture layer seems to be significantly deeper than shown in the model simulations (about 250 hPa deep vs. 150 hPa).

The 18 UTC sounding at KAMA was considered too far away from the airmass boundary (≈160 km from KLBB) to accurately represent the cool side environment, which is the reason this sounding was not considered for this study. In addition, it has not been shown in published literature that low-level moisture has a significant impact on supercell morphology; it is more likely due to upper-level storm relative winds (Moller et al. 1990, Rasmussen and Straka 1998) or interaction with surrounding convection (Kulie and Lin 1998, Finley et al. 2001). In the case study, the supercell became HP after numerous mergers with surrounding convection, which was not present in the simulation and is likely the reason for the difference in storm morphology observed.

Moller, A. R., C. A. Doswell III, and R. Przybylinski, 1990: High-precipitation supercells: A conceptual model and documentation. Preprints, 16th Conf. on Severe Local Storms, *Kananaskis Park, AB, Canada, Amer. Meteor. Soc., 52–57.*

Kulie, M. S., and Y.-L. Lin, 1998: The structure and evolution of a numerically simulated high-precipitation supercell thunderstorm. Mon. Wea. Rev., ***126****, 2090–2116.*

Rasmussen, E. N., and J. M. Straka, 1998: Variations in supercell morphology. Part I: Observations of the role of upper-level storm-relative flow. Mon. Wea. Rev., ***126****, 2406–2421.*

Finley, C. A., W. R. Cotton, R. A. Pielke, 2001: Numerical simulation of tornadogenesis in a high-precipitation supercell. Part I: Storm evolution and transition into a bow echo. J. Atmos. Sci., ***58****, 1597–1629.*

GENERAL NOTE: I feel that this paper provides a valuable addition to the literature regarding supercells and their environments. The methodology utilizing a high-resolution idealized model seems well-designed and thorough. While the specific results are applicable only to this case, I believe the authors present sufficient evidence that some general conclusions can be made about the behavior of supercells interacting with baroclinic boundaries and that perhaps with additional sensitivity studies, operationally employable predictions might be possible.

GENERAL NOTE: The use of some vague descriptive terms (i.e. profound, dramatic, much more, etc) instead of more specific, quantitative ones may slightly diminish the scientific veracity of the paper. Any adjustments to these terms by the authors to increase specificity would likely result in an improved final product.

FINAL NOTE: Many of my "suggested" changes to words and phrases are based solely on personal preference. I don't expect that the authors will feel compelled to make all those changes – they are truly just suggestions.

[Minor comments omitted...]

Second review:

Recommendation: Accept.

Overview: I read through much of the manuscript last night, and it looks very good to me; so far all of my "concerns" have been addressed. I'm okay with not conducting a [third] review. If I notice any typos or anything, I'll let you know.

Thanks again for letting me be part of the review team.